 CMES, vol.8, no.3, pp.231-258, 2005

Computational Applications of the Poincaré Group on the Elastoplasticity with Kinematic Hardening

Chein-Shan Liu [1]

Abstract: Using a group-theoretical approach in the Minkowski space we explore kinematic hardening rules from a viewpoint of the Poincaré group. The resultant models possess two intrinsic times q_0^a and q_0^b; the first q_0^a controls the on/off switch of plasticity, and the second q_0^b controls the pace of back stress during plastic deformation. We find that some existent kinematic hardening rules, including the modifications from the Armstrong-Frederick kinematic hardening rule, can be categorized into type I, type II and type III, which correspond respectively to $q_0^b = 0$, $q_0^b = q_0^a$ and $q_0^b \neq q_0^a$. Based on group properties, the numerical computations of models' responses are derived, which can automatically update the stress points located on the yield surface at every time step without needing of iteration, and some examples are plotted to show models' behaviors.

keyword: Elastoplasticity, kinematic hardening rule, Poincaré group, numerical computation, Minkowski space

1 Introduction

Group theory as a mathematical tool to study symmetry has an abundance of applications from various fields. Numerous problems in engineering sciences possess certain symmetry properties. If we can manage to recognize them, a mathematical treatment adjusted to the symmetry properties may lead to a considerable simplification.

With this in mind, internal symmetries approach of the elastoplastic models equipped with the von Mises yield criterion have been developed by Hong and Liu (1999a, 2000), Liu and Hong (2001), Mukherjee and Liu (2003), and Liu (2001a, 2003a, 2004a, 2004b). Then, Liu (2004c) and Liu and Chang (2004, 2005) extended these studies to the Drucker-Prager model, quadratic yielding model and convex plastic model. These authors explored the internal symmetry groups of the constitutive models of perfect elastoplasticity with or without considering large deformation, visco-elastoplasticity, isotropic work-hardening elastoplasticity, mixed-hardening elastoplasticity, the Drucker-Prager plasticity as well as the models with yield functions quadratic or convex, to ensure that the consistency condition is exactly satisfied at each time step once the computational schemes can take these symmetries into account.

The perfectly plastic model is the simplest one to use (Hong and Liu, 1997, 1998), but can't predict the experimentally observed Bauschinger effect of most metals in cyclic loading tests. The Bauschinger effect refers to a particular type of directional anisotropy in stress space induced by plastic deformation: an initial plastic deformation of one direction reduces the subsequent yield strength in the opposite direction. To model the Bauschinger effect, both Ishlinsky (1954) and Prager (1955, 1956) simultaneously suggested the kinematic hardening rule. This rule asserts that the yield surface translates as a rigid body in stress space during plastic deformation. Consequently, the shape and size of yield surface remain unchanged in the subsequent plastic deformation.

Although the kinematic hardening rule proposed by Prager can account of the Bauschinger effect within a certain degree of accuracy, the difficulties appear when applied it to model the realistic material behavior under complex loading conditions. The main drawback of Prager's kinematic hardening rule is that the back stress doesn't saturate. Then, Armstrong and Frederick (1966) have proposed a kinematic hardening rule modified from the Prager kinematic hardening rule by adding a recovery term in the governing differential equation of back stress. There are several reasons to adopt the Armstrong-Frederick kinematic hardening rule in the modeling of cyclic plasticity (Moosbrugger and Morrison, 1997; Chaboche, 1993; McDowell, 1985; Moos-

[1] Department of Mechanical and Mechatronic Engineering, Taiwan Ocean University, Keelung, Taiwan, E-mail: csliu@mail.ntou.edu.tw

brugger and McDowell, 1989; Moosbrugger, 1993; McDowell and Moosbrugger, 1992; Ohno and Wang, 1991): able to be incorporated into a thermodynamical frame, able to model nonlinear uniaxial Bauschinger effect, able to model nonproportional strain loading response, connecting to a micromechanical process, and more significantly having a connection to the two-surface and multiple-surface models. On the other hand, there are also several numerical schemes been developed to integrate the Armstrong-Frederick model, for example, Lubarda and Benson (2002), Wang, Hu and Sawyer (2000), Sawyer, Wang and Jones (2001), Chaboche and Cailletaud (1996), and Liu and Li (2005).

However, in order to increase the prediction capability of the models which using back stress to simulate the hardening phenomena of materials, many nonlinear kinematic hardening rules have been proposed in the past several decades. One of these efforts is that the model proposed by Armstrong and Frederick (1966) has been extended and refined through the works of Eisenberg and Phillips (1968), Chaboche (1977, 1986, 1989, 1991, 1994), Voyiadjis and Kattan (1990,1991), Ohno and Wang (1993, 1994), Jiang and Kurath (1996), Moosbrugger and Morrison (1997), and so on. Sometimes, the kinematic hardening effect is also important in the finite strain plasticity model (Atluri, 1984; Im and Atluri, 1987; Karšaj, Sansour and Sorić, 2005).

Hong and Liu (1999b) have investigated the constitutive model of bilinear elastoplasticity by using the method of symmetry group. In doing so they have found that the internal symmetry inherent in the Prager model is a Poincaré group on the Minkowski space. On the other hand, Hong and Liu (2001a) have distilled a perfectly plastic model from a primitive model that the Lorentz group admitted by enforcing two basic principles of plasticity: causality in the truncated future cone of the Minkowski spacetime of augmented states, and controllability and non-generativity in a reachable, bounded space of states. In addition these studies, there are no reports in the open literature to investigate the plasticity models endowed with nonlinear kinematic hardening rules from a group-theoretic approach and the computations by utilizing the symmetry groups. To benefit a symmetry study of mechanical problems, we attempt to investigate the kinematic hardening models of elastoplasticity from a viewpoint of the Poincaré group, and utilize the group properties to facilitate the computations of models' behaviors.

The most models developed are based on one intrinsic time of the conventional types as discussed by Watanabe and Atluri (1986) and Im and Atluri (1987). In this paper one will find that the introduction of two intrinsic times in the theory of plasticity is a very natural result from the viewpoint of Poincaré group. The nonlinear kinematic hardening models advocated by Chaboche (1994) and Ohno and Wang (1993, 1994) can be covered. They are the modifications of the Armstrong-Frederick kinematic hardening rule to suppress the over dynamic recovery effect of back stress.

This paper is arranged as follows. In Section 2 we start from a Poincaré group to derive the flow model, which not only considers the effect of kinematic hardening but also accounts of large deformation effect. In Section 3 the models with two intrinsic times are given and then compared with some existent elastoplastic models with nonlinear kinematic hardening rules. In Section 4 we address the numerical computations of the newly proposed models. In Section 5 we introduce a smoothing technique developed by Liu (2003b) to improve the model behavior. Then, we draw some conclusions in Section 6.

The concept of internal spacetime as advocated by Hong and Liu (1999a, 1999b, 2000) to model materials' plastic behaviors bears certain similarities with the external spacetime structure originated from the Einstein's landmark theory of special relativity (Hong and Liu, 2001b). Both spacetimes are of the Minkowskian type and the action groups are both of the Lorentzian type, but with different dimensions.

Through this study it would be clear that these seeming diverse kinematic hardening rules can be unified into a single equation in the Minkowski space, of which the group action is a Poincaré group. This group extends the action of the Lorentz group, allowing the cone moving in the material internal spacetime. The new aspect may extend the conventional internal time concept of plasticity (Watanabe and Atluri, 1986; Im and Atluri, 1987) to an internal spacetime concept of plasticity. So far, we can study plasticity theory from a highlight of materials' spacetime structure.

2 Poincaré group: the model with corotational stress rate and kinematic hardening

As the title indicates, let us first give a brief sketch of the Poincaré group in this section. We attempt to construct a causal differential equations system in an appropriate space, on which the temporal component flows forward and causes precede effects. Zeeman (1964) was able to show that the causality assumption in the Minkowski spacetime renders a composition of a translation, a dilation, and a proper orthochronous Lorentz transformation. In the present paper we will focus on the composition of a translation and a proper orthochronous Lorentz transformation.

2.1 The Poincaré group and its Lie algebra

It is known that the semi-direct product of the translation group $T(n,1)$ with the proper orthochronous Lorentz group $SO_o(n,1)$ results in the proper orthochronous Poincaré group $ISO_o(n,1)$, of which $T(n,1)$ is an invariant subgroup and $SO_o(n,1)$ is a proper subgroup. An element of $ISO_o(n,1)$ is a pair of linear operators $\{\mathbf{X}_b|\mathbf{G}\}$ with $\mathbf{X}_b \in T(n,1)$ and $\mathbf{G} \in SO_o(n,1)$ satisfying (Liu, 2001b)

$$\mathbf{G}^T\mathbf{g}\mathbf{G} = \mathbf{g}, \tag{1}$$

$$\det \mathbf{G} = 1, \tag{2}$$

$$G_0^0 > 0, \tag{3}$$

in which the superscript T denotes the transpose, det is the shorthand of determinant, G_0^0 is the 00th component of $\mathbf{G}$ and

$$\mathbf{g} := \begin{bmatrix} \mathbf{I}_n & \mathbf{0}_{n\times 1} \\ \mathbf{0}_{1\times n} & -1 \end{bmatrix} \tag{4}$$

is a metric tensor of the Minkowski space $\mathbb{M}^{n+1}$. In above, $\mathbf{I}_n$ is the identity matrix of order n. It deserves to note that the 00th component of $\mathbf{g}$ is -1 rather than $+1$ for the metric tensor $\mathbf{I}_{n+1}$ of the $n+1$-dimensional Euclidean space $\mathbb{E}^{n+1}$. The action of $ISO_o(n,1)$ on $\mathbb{M}^{n+1}$ is a Lorentz transformation $\mathbf{G}$ followed by a translation $\mathbf{X}_b$:

$$\mathbf{X}(t) = \{\mathbf{X}_b(t)|\mathbf{G}(t)\}\mathbf{X}(0) := \mathbf{G}(t)\mathbf{X}(0) + \mathbf{X}_b(t). \tag{5}$$

Here, t is a parameter, and the group formulated is a single-parameter subgroup. Using this formula the multiplication and inversion of group actions in $ISO_o(n,1)$ are found to be

$$\begin{aligned}&\{\mathbf{X}_b(t_2)|\mathbf{G}(t_2)\}\{\mathbf{X}_b(t_1)|\mathbf{G}(t_1)\}\\ &\quad=\{\mathbf{G}(t_2)\mathbf{X}_b(t_1)+\mathbf{X}_b(t_2)|\mathbf{G}(t_2)\mathbf{G}(t_1)\},\end{aligned} \tag{6}$$

$$\{\mathbf{X}_b(t)|\mathbf{G}(t)\}^{-1} = \{-\mathbf{G}^{-1}(t)\mathbf{X}_b(t)|\mathbf{G}^{-1}(t)\}, \tag{7}$$

for all $\mathbf{G}(t_1), \mathbf{G}(t_2), \mathbf{G}(t) \in SO_o(n,1)$ and $\mathbf{X}_b(t_1), \mathbf{X}_b(t_2), \mathbf{X}_b(t) \in T(n,1)$.

In order to derive the commutation relations of the real Lie algebra of $ISO_o(n,1)$ it is convenient embedding $ISO_o(n,1)$ into the special linear group $SL(n+2,\mathbb{R})$ via the following mapping:

$$\{\mathbf{X}_b(t)|\mathbf{G}(t)\} \mapsto \begin{bmatrix} \mathbf{G}(t) & \mathbf{X}_b(t) \\ \mathbf{0}_{1\times(n+1)} & 1 \end{bmatrix}. \tag{8}$$

Thus, the operation in Eq. (5) can be recast to the following matrix Lie group operation:

$$\begin{bmatrix} \mathbf{X}(t) \\ 1 \end{bmatrix} = \begin{bmatrix} \mathbf{G}(t) & \mathbf{X}_b(t) \\ \mathbf{0}_{1\times(n+1)} & 1 \end{bmatrix} \begin{bmatrix} \mathbf{X}(0) \\ 1 \end{bmatrix}, \tag{9}$$

which can be further split into

$$\begin{bmatrix} \mathbf{X}(t) \\ 1 \end{bmatrix} = \Big(\mathbf{T}(t)|\mathbf{L}(t)\Big) \begin{bmatrix} \mathbf{X}(0) \\ 1 \end{bmatrix} \tag{10}$$

with $\Big(\mathbf{T}(t)|\mathbf{L}(t)\Big)$ denoting the matrix multiplication of $\mathbf{T}(t)$ and $\mathbf{L}(t)$:

$$\begin{aligned}\mathbf{T}(t) &:= \begin{bmatrix} \mathbf{I}_{n+1} & \mathbf{X}_b(t) \\ \mathbf{0}_{1\times(n+1)} & 1 \end{bmatrix},\\ \mathbf{L}(t) &:= \begin{bmatrix} \mathbf{G}(t) & \mathbf{0}_{(n+1)\times 1} \\ \mathbf{0}_{1\times(n+1)} & 1 \end{bmatrix}.\end{aligned} \tag{11}$$

This group action has the following algebraic properties:

$$\mathbf{T}(t_1)\mathbf{T}(t_2) = \mathbf{T}(t_2)\mathbf{T}(t_1), \tag{12}$$

$$\begin{aligned}&\big(\mathbf{T}(t_2)|\mathbf{L}(t_2)\big)\big(\mathbf{T}(t_1)|\mathbf{L}(t_1)\big)\\ &\quad= \Big(\mathbf{T}(t_2)\mathbf{L}(t_2)\mathbf{T}(t_1)\mathbf{L}^{-1}(t_2)|\mathbf{L}(t_2)\mathbf{L}(t_1)\Big).\end{aligned} \tag{13}$$

The former indicates that $\mathbf{T}(t)$ is an invariant subgroup of the Poincaré group, and the latter shows that the reason why the Poincaré group is a semi-direct product of the translation group and the Lorentz group. Both $\mathbf{T}(t)$ and $\mathbf{L}(t)$ are non-compact, and so is the Poincaré group. Because $\mathbf{T}(t)$ is an abelian subgroup, the Poincaré group is not semi-simple.

The real Lie algebra $iso(n,1)$ of the Poincaré group $ISO_o(n,1)$ is most easily set up by using $\mathbf{T}(t)$ and $\mathbf{L}(t)$ defined above. Now, by adopting the argument of elementary responses as for the Lorentz group derived in a previous paper (Section 10 in Hong and Liu, 1999a), the basis elements of $iso(n,1)$ are given as follows. The $n(n+1)/2$ basis elements of the real Lie algebra $iso(n,1)$ corresponding to the homogeneous Lorentz group is of the form

$$\mathbf{l}_{ij} := \begin{bmatrix} \mathbf{a}_{ij} & \mathbf{0}_{(n+1)\times 1} \\ \mathbf{0}_{1\times(n+1)} & 0 \end{bmatrix}, \tag{14}$$

where $\mathbf{a}_{ij}$, $0 \le i < j \le n$, is the basis elements of the real Lie algebra of the Lorentz group $SO_o(n,1)$ with

$$\mathbf{a}_{ij} := \begin{bmatrix} & \vdots & & \vdots & \\ \cdots & . & \cdots & 1 & \cdots \\ & \vdots & & \vdots & \\ \cdots & -1 & \cdots & . & \cdots \\ & \vdots & & \vdots & \end{bmatrix} \tag{15}$$

for $1 \le i < j \le n$, and with n basis elements of the type

$$\mathbf{a}_{i0} := \begin{bmatrix} & \vdots & & \vdots \\ \cdots & . & \cdots & 1 \\ & \vdots & & \vdots \\ \cdots & 1 & \cdots & . \end{bmatrix} \tag{16}$$

for $1 \le i \le n$. Similarly, the $n+1$ basis elements of the Lie algebra $iso(n,1)$ corresponding to the translation is given by

$$\mathbf{k}_i := \begin{bmatrix} & \vdots & & \vdots \\ \cdots & . & \cdots & 1 \\ & \vdots & & \vdots \\ \cdots & & \cdots & . \end{bmatrix} \tag{17}$$

for $0 \le i \le n$, where $\mathbf{k}_i$ is equal to $\mathbf{0}_{(n+2)\times(n+2)}$ except that the ith entry of the last column is $+1$.

The basis elements (14) and (17) obey the commutation relations

$$\begin{aligned} &[\mathbf{l}_{ij}, \mathbf{l}_{kl}] = \eta_{jk}\mathbf{l}_{il} + \eta_{il}\mathbf{l}_{jk} - \eta_{ik}\mathbf{l}_{jl} - \eta_{jl}\mathbf{l}_{ik}, \\ &[\mathbf{l}_{ij}, \mathbf{k}_k] = \eta_{ik}\mathbf{k}_j - \eta_{jk}\mathbf{k}_i, \\ &[\mathbf{k}_i, \mathbf{k}_j] = \mathbf{0} \end{aligned} \tag{18}$$

for $i, j, k, l = 1, 2, \ldots, n, 0$, with η defined by

$$\eta := \begin{bmatrix} \mathbf{g} & \mathbf{0}_{(n+1)\times 1} \\ \mathbf{0}_{1\times(n+1)} & 1 \end{bmatrix}. \tag{19}$$

Any continuous square matrix function $\mathbf{B}(t) \in iso(n,1)$ of order $n+1$ is thus a linear combination of the basis elements (14) and (17):

$$\mathbf{B}(t) = \sum_{0\le i<j\le n} A^{ij}(t)\mathbf{l}_{ij} + \sum_{0\le i\le n} K^i(t)\mathbf{k}_i \tag{20}$$

with entries $A^{ij} = -A^{ji}$ for $1 \le i \le j \le n$, $A^{i0} = A^{0i}$ for $1 \le i \le n$ and $A^{00} = 0$. Consequently, we have a single-parameter linear differential equations system with the coefficient matrix $\mathbf{B}$:

$$\begin{aligned} \frac{d}{dt}\begin{bmatrix} \mathbf{X}(t) \\ 1 \end{bmatrix} &= \mathbf{B}(t)\begin{bmatrix} \mathbf{X}(t) \\ 1 \end{bmatrix} \\ &= \begin{bmatrix} \mathbf{A}(t) & \mathbf{K}(t) \\ \mathbf{0}_{1\times(n+1)} & 0 \end{bmatrix}\begin{bmatrix} \mathbf{X}(t) \\ 1 \end{bmatrix}. \end{aligned} \tag{21}$$

Taking the above first row leads to

$$\dot{\mathbf{X}}(t) = \mathbf{A}(t)\mathbf{X}(t) + \mathbf{K}(t), \tag{22}$$

where both $\mathbf{A}(t)$ and $\mathbf{K}(t)$ are continuous functions.

2.2 A causal system

From Eq. (5) it follows that

$$\mathbf{X}(t_1) = \mathbf{G}(t_1)\mathbf{X}(0) + \mathbf{X}_b(t_1), \tag{23}$$

for some parameter t_1. Substituting the inverse of the above equation for $\mathbf{X}(0)$ into Eq. (5) again we obtain

$$\begin{aligned} \mathbf{X}(t) = &[\mathbf{G}(t)\mathbf{G}^{-1}(t_1)]\mathbf{X}(t_1) + \mathbf{X}_b(t) \\ &- [\mathbf{G}(t)\mathbf{G}^{-1}(t_1)]\mathbf{X}_b(t_1). \end{aligned} \tag{24}$$

Owing to the closure property of the Lie group, $[\mathbf{G}(t)\mathbf{G}^{-1}(t_1)]$ also belongs to $SO_o(n,1)$. When t_1 is put very close to t, $[\mathbf{G}(t)\mathbf{G}^{-1}(t_1)]$ is very close to the identity of $SO_o(n,1)$; moreover, in view of Eqs. (2) and (3), the group manifold is analytic, and hence,

$$\mathbf{A}(t) := \frac{\partial}{\partial t}[\mathbf{G}(t)\mathbf{G}^{-1}(t_1)]\bigg|_{t_1=t} = \dot{\mathbf{G}}(t)\mathbf{G}^{-1}(t) \tag{25}$$

defines a string of tangent vectors on the tangent space at the identity of the group manifold, more precisely, a continuously-singly-parametrized series of one-dimensional subalgebra of the real Lie algebra $so(n,1)$ of the Lorentz group $SO_o(n,1)$.

Differentiating Eqs. (1) and (24), setting $t_1 = t$, and then using Eq. (25) yield

$$\mathbf{A}^T\mathbf{g} + \mathbf{g}\mathbf{A} = \mathbf{0}, \tag{26}$$

$$\dot{\mathbf{X}}(t) = \mathbf{A}(t)\mathbf{X}(t) + \dot{\mathbf{X}}_b(t) - \mathbf{A}(t)\mathbf{X}_b(t). \tag{27}$$

The flow generated by such an $iso(n,1)$ is the congruence of curves resulting from solving the dynamical system (27). Due to Eq. (25), $\mathbf{G}(t)$ is the fundamental solution of the system of ordinary differential equations (27). From Eq. (26), $\mathbf{gA}$ is skew-symmetric; and, therefore, we may let

$$\mathbf{A} := \begin{bmatrix} \mathbf{\Omega} & \frac{\dot{\boldsymbol{q}}}{q_y} \\ \frac{\dot{\boldsymbol{q}}^T}{q_y} & 0 \end{bmatrix}, \tag{28}$$

where $\mathbf{\Omega}$ is a skew-symmetric spin tensor, $q_y := Q_a^0/k_e$ is the yield strain, and $k_e > 0$ and $Q_a^0 > 0$ are respectively the elastic modulus and yield stress. Refer Eq. (36a) in Hong and Liu (1999a).

Comparing Eqs. (27) and (22) yields

$$\dot{\mathbf{X}}_b(t) = \mathbf{A}(t)\mathbf{X}_b(t) + \mathbf{K}(t). \tag{29}$$

On the other hand, if we let

$$\mathbf{X}_a(t) := \mathbf{X}(t) - \mathbf{X}_b(t) \tag{30}$$

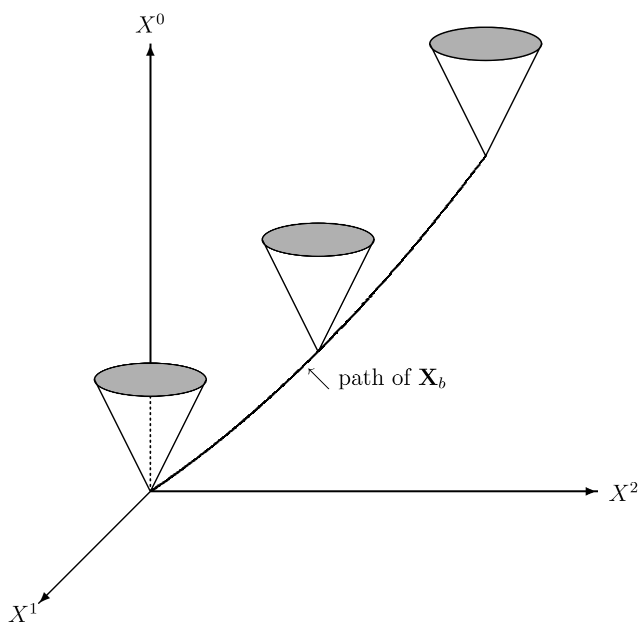

Figure 1 : Moving cones with vertex $\mathbf{X}_b$ in the augmented state space, the translation of the vertex point is due to kinematic hardening in the state space of $\mathbf{Q}$.

in Eq. (24), then we obtain

$$\mathbf{X}_a(t) = [\mathbf{G}(t)\mathbf{G}^{-1}(t_1)]\mathbf{X}_a(t_1). \tag{31}$$

By the same token, when differentiating the above equation with respect to t, setting $t_1 = t$, and then using Eq. (25) we obtain

$$\dot{\mathbf{X}}_a(t) = \mathbf{A}(t)\mathbf{X}_a(t). \tag{32}$$

From Eqs. (1) and (31) it is easy to prove that

$$\mathbf{X}_a^T(t)\,\mathbf{g}\,\mathbf{X}_a(t) = \mathbf{X}_a^T(t_1)\mathbf{g}\mathbf{X}_a(t_1) \tag{33}$$

is an invariant; hence, we suppose that

$$\mathbf{X}_a^T\,\mathbf{g}\,\mathbf{X}_a = -r, \tag{34}$$

where $r < 1$ is a material constant specifying the isotropic hardening. It is a hyperboloid, an n-dimensional pseudo-Riemannian submanifold of constant curvature, which admits the Minkowski metric. If the constant $r = 0$, Eq. (34) is *the cone*, whose vertex point $\mathbf{X}_b$ can move in the space of $\mathbf{X}$; see Fig. 1. If $r > 0$, it represents two copies of the Minkowskian spheres in *the interior*. If $r < 0$, it is a hyperbolic space in *the exterior*. Figure 2 shows a geometric representation of the above three objects. In Section 5 we will consider a smoothing model whose underlying space is an interior upper hyperboloid in the Minkowski sphere.

2.3 A mathematical model in the space of X

The flows equations (22), (32) and (29) derived in the space of $(\mathbf{X}, \mathbf{X}_a, \mathbf{X}_b)$ were based on the Poincaré group, collected together as follows:

$$\dot{\mathbf{X}} = \mathbf{AX} + \mathbf{K}, \tag{35}$$

$$\dot{\mathbf{X}}_a = \mathbf{AX}_a, \tag{36}$$

$$\dot{\mathbf{X}}_b = \mathbf{AX}_b + \mathbf{K}. \tag{37}$$

The problems encountered in the engineering applications are often posed as follows. Given a set of controls, $\dot{\mathbf{q}}$ and $\mathbf{\Omega}$ as given in $\mathbf{A}$ by Eq. (28), and a vector source function of the translation $\mathbf{K}$, find the response state of $\mathbf{X}$. For the given $\mathbf{A}$ and $\mathbf{K}$ it is a matter to solve the non-homogeneous differential equation system (35). Usually, we search a *complementary solution* of Eq. (36) denoted by $\mathbf{X}_a$ and then a *particular solution* of Eq. (37) denoted

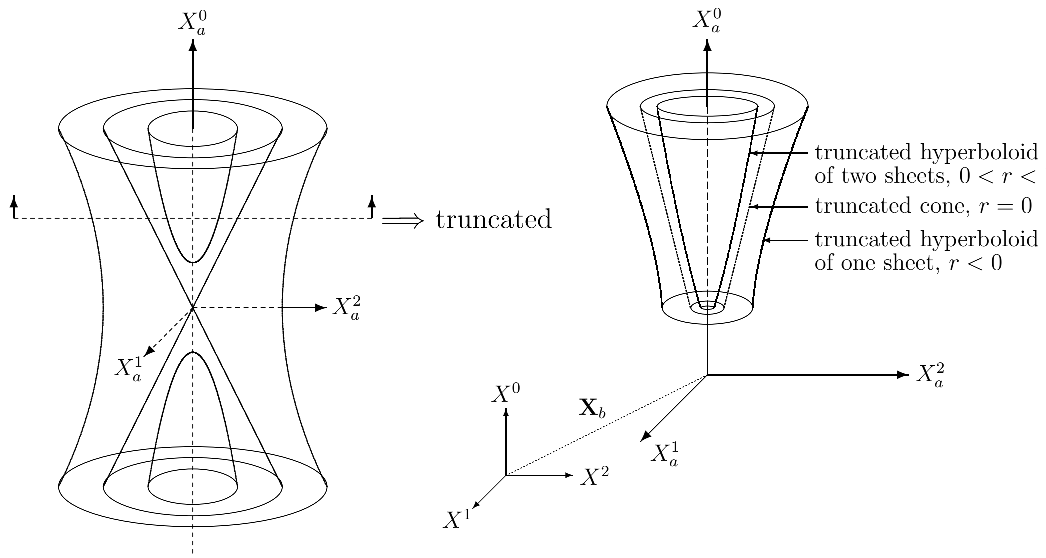

Figure 2 : The three geometric sets of $\mathbf{X}_a^T \mathbf{g} \mathbf{X}_a = -r$ and $X_a^0 \geq 1$. Depending on the value of r the set is truncated hyperboloid of two sheets, truncated cone, or truncated hyperboloid of one sheet.

by $\mathbf{X}_b$, and thus the *general solution* $\mathbf{X}$ of Eq. (35) is expressed as the following sum of *complementary solution* and *particular solution*:

$$\mathbf{X} = \mathbf{X}_a + \mathbf{X}_b. \tag{38}$$

The above equations constitute a *two-layer* system: Eq. (36) is the first layer and Eq. (37) is the second layer. Whatever, how to identify the source function of the translation $\mathbf{K}$ becomes a major task in the material modeling of kinematic hardening. Because $\mathbf{A}$ is an input and $\mathbf{X}_a$ is an output of the first layer obtained by solving Eq. (36) with a prescribed initial condition $\mathbf{X}_a(t_i)$, it is reasonable to let

$$\mathbf{K} = \mathbf{K}(\mathbf{A}, \mathbf{X}_a, \mathbf{X}_b). \tag{39}$$

The dependence of $\mathbf{K}$ on $\mathbf{X}_b$ is for considering the nonlinear effect of $\mathbf{X}_b$ through the differential equation (37) and for reflecting the nonlinear kinematic hardening effect to be discussed below. It can be seen that $\mathbf{K}$ not only depends on the control inputs of Ω and $\dot{\mathbf{q}}$ but also the output of the first layer of the system: q_0^a, $\mathbf{Q}_a$. Therefore, $\mathbf{K}$ depends on the rate and history of the inputs. The two-layer structure is schematically shown in Fig. 3.

The model of plasticity is known as rate-independent. The stress response depends on the strain path but is independent of what strain rate on the path. Let us consider two independent variables t and t', where t and t' have a monotonic relation, *i.e.*, $dt'/dt > 0$. To be a rate-independent plasticity model $\mathbf{K}$ and $\mathbf{A}$ should be also rate-independent as degree-one homogeneous functions of rate quantities:

$$\mathbf{A}(t')dt' = \mathbf{A}(t)dt, \tag{40}$$
$$\mathbf{K}(t')dt' = \mathbf{K}(t)dt. \tag{41}$$

Multiplying Eqs. (35)-(37) by dt/dt' we get the same equations:

$$\frac{d}{dt'}\mathbf{X}(t') = \mathbf{A}(t')\mathbf{X}(t') + \mathbf{K}(t'), \tag{42}$$
$$\frac{d}{dt'}\mathbf{X}_a(t') = \mathbf{A}(t')\mathbf{X}_a(t'), \tag{43}$$
$$\frac{d}{dt'}\mathbf{X}_b(t') = \mathbf{A}(t')\mathbf{X}_b(t') + \mathbf{K}(t'), \tag{44}$$

but with a dependence on t replaced merely by a dependence on t' of $\mathbf{X}$, $\mathbf{X}_a$ and $\mathbf{X}_b$. Therefore, both t and t' can be equally well the independent variable of plasticity equations, and it makes no distinction between the use of t or t'. However, for convenience, the independent variable no matter what it is will be simply called "time" and given the symbol t.

The $\boldsymbol{\Omega}$ appeared in $\mathbf{A}$ is a skew-symmetric tensor reflecting the corotational rates used in the model; see, *e.g.*, Liu and Hong (1999, 2001) and references therein. Since the dependence of $\boldsymbol{\Omega}$ on t is through the deformation rate of

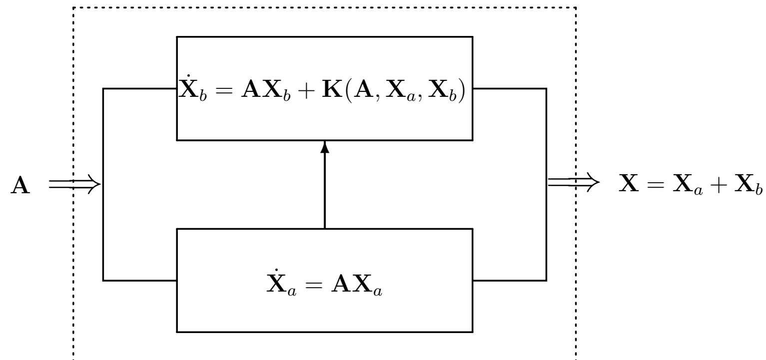

Figure 3 : A two-layer structure of the input and output relations of the augmented linear systems based on the Poincaré group theory.

material, $\mathbf{\Omega}$ and $\mathbf{A}$ are both rate-independent.

2.4 A mathematical model in the space of $\mathbf{Q}$

In the following sections we focus on the complex problem of kinematic hardening plasticity, restrict ourselves to a small strain theory and thus not consider the finite strain plasticity as discussed by Atluri (1984), Im and Atluri (1987) and Karšaj, Sansour and Sorić (2005).

The spaces we work are five-dimensional stress and strain vector spaces (Liu 2003a):

$$\mathbf{Q} = \begin{bmatrix} a_1 s^{11} + a_2 s^{22} \\ a_3 s^{11} + a_4 s^{22} \\ s^{23} \\ s^{13} \\ s^{12} \end{bmatrix}, \mathbf{Q}_a = \begin{bmatrix} a_1 s_a^{11} + a_2 s_a^{22} \\ a_3 s_a^{11} + a_4 s_a^{22} \\ s_a^{23} \\ s_a^{13} \\ s_a^{12} \end{bmatrix},$$

$$\mathbf{Q}_b = \begin{bmatrix} a_1 s_b^{11} + a_2 s_b^{22} \\ a_3 s_b^{11} + a_4 s_b^{22} \\ s_b^{23} \\ s_b^{13} \\ s_b^{12} \end{bmatrix}, \tag{45}$$

$$\mathbf{q} = \begin{bmatrix} a_1 e_{11} + a_2 e_{22} \\ a_3 e_{11} + a_4 e_{22} \\ e_{23} \\ e_{13} \\ e_{12} \end{bmatrix}, \mathbf{q}^e = \begin{bmatrix} a_1 e_{11}^e + a_2 e_{22}^e \\ a_3 e_{11}^e + a_4 e_{22}^e \\ e_{23}^e \\ e_{13}^e \\ e_{12}^e \end{bmatrix},$$

$$\mathbf{q}^p = \begin{bmatrix} a_1 e_{11}^p + a_2 e_{22}^p \\ a_3 e_{11}^p + a_4 e_{22}^p \\ e_{23}^p \\ e_{13}^p \\ e_{12}^p \end{bmatrix}. \tag{46}$$

They are independent components of $\mathbf{s}$, $\mathbf{s}_a$, $\mathbf{s}_b$ $\mathbf{e}$, $\mathbf{e}^e$ and $\mathbf{e}^p$, which are, respectively, the deviatoric tensors of stress, active stress, back stress, strain, elastic strain, and plastic strain, all symmetric and traceless.

In Eqs. (44)-(49),

$$\begin{aligned} a_1 &:= \sin(\theta + \frac{\pi}{3}), \\ a_2 &:= \sin\theta, \\ a_3 &:= \cos(\theta + \frac{\pi}{3}), \\ a_4 &:= \cos\theta, \end{aligned} \tag{47}$$

where θ can be any real number. If choosing $\theta = 0$ we have the stress space $\mathbf{Q} := (\sqrt{3}s^{11}/2, s^{11}/2 + s^{22}, s^{23}, s^{13}, s^{12})^T$ of the Il'yushin type (Hong and Liu, 1997).

Depending on the number of non-zero stress components in Eq. (45) (and correspondingly non-zero strain components in Eq. (46)) which we consider for a physical problem, for example, the simple shear problem, the axial tension-compression problem, the biaxial tension-compression-torsion problem, etc., the dimensions n may be an integer with $1 \le n \le 5$, and no matter which case is we use n to denote the physical problem dimensions.

In order to transform the differential equations in the space of $(\mathbf{X}, \mathbf{X}_a, \mathbf{X}_b)$ to the flow model in the space of

$(\mathbf{Q}, \mathbf{Q}_a, \mathbf{Q}_b, q_0^a, q_0^b)$ we need the following projective relations between these two sets:

$$\mathbf{X}_a = \begin{bmatrix} \mathbf{X}_a^s \\ X_a^0 \end{bmatrix} := X_a^0 \begin{bmatrix} \frac{\mathbf{Q}_a}{Q_a^0} \\ 1 \end{bmatrix} = \exp\left(\frac{k_a q_0^a}{Q_a^0}\right) \begin{bmatrix} \frac{\mathbf{Q}_a}{Q_a^0} \\ 1 \end{bmatrix}, \tag{48}$$

$$\mathbf{X}_b = \begin{bmatrix} \mathbf{X}_b^s \\ X_b^0 \end{bmatrix} := X_b^0 \begin{bmatrix} \frac{\mathbf{Q}_b}{Q_b^0} \\ 1 \end{bmatrix} = \exp\left(\frac{k_b q_0^b}{Q_b^0}\right) \begin{bmatrix} \frac{\mathbf{Q}_b}{Q_b^0} \\ 1 \end{bmatrix}. \tag{49}$$

The above representations include four material constants of Q_a^0, Q_b^0, k_a and k_b and two time-like variables of q_a^0 and q_b^0 to be discussed below. Corresponding to the elastic modulus $k_e > 0$, we may call $k_b > 0$ the kinematic modulus and $k_a := k_e + k_b > 0$ the active modulus.

From the above two definitions it follows that

$$\mathbf{Q}_a = \frac{Q_a^0 \mathbf{X}_a^s}{X_a^0}, \tag{50}$$

$$\mathbf{Q}_b = \frac{Q_b^0 \mathbf{X}_b^s}{X_b^0}, \tag{51}$$

$$\mathbf{Q} = \mathbf{Q}_a + \mathbf{Q}_b = \frac{Q_a^0 \mathbf{X}_a^s}{X_a^0} + \frac{Q_b^0 \mathbf{X}_b^s}{X_b^0}, \tag{52}$$

$$\dot{q}_0^a = \frac{Q_a^0 \dot{X}_a^0}{k_a X_a^0}, \tag{53}$$

$$\dot{q}_0^b = \frac{Q_b^0 \dot{X}_b^0}{k_b X_b^0}, \tag{54}$$

where $\mathbf{X}_a^s = (X_a^1, X_a^2, \ldots, X_a^n)^T$ and $\mathbf{X}_b^s = (X_b^1, X_b^2, \ldots, X_b^n)^T$ are respectively the n-vector parts of $\mathbf{X}_a$ and $\mathbf{X}_b$, and X_a^0 and X_b^0 are respectively the scalar parts of $\mathbf{X}_a$ and $\mathbf{X}_b$. By definitions we have $X_a^0 > 0$ and $X_b^0 > 0$. Corresponding to Eq. (38) in the space of $\mathbf{X}$, Eq. (52) represents an usual decomposition of stress $\mathbf{Q}$ into an active (relative) stress $\mathbf{Q}_a$ and a back stress $\mathbf{Q}_b$. Eq. (53) is obtained by taking the differential of $q_0^a = Q_a^0/k_a \ln X_a^0$, and Eq. (54) is obtained by taking the differential of $q_0^b = Q_b^0/k_b \ln X_b^0$.

Now, utilizing Eqs. (36), (37), (48), (49), (28), (53) and (54) we obtain

$$\overset{\circ}{\mathbf{Q}}_a + \frac{k_a \dot{q}_0^a}{Q_a^0} \mathbf{Q}_a = k_e \dot{\mathbf{q}}, \tag{55}$$

$$\dot{q}_0^a = \frac{k_e}{k_a Q_a^0} \mathbf{Q}_a^T \dot{\mathbf{q}}, \tag{56}$$

$$\overset{\circ}{\mathbf{Q}}_b + \frac{k_b \dot{q}_0^b}{Q_b^0} \mathbf{Q}_b = \frac{k_e Q_b^0}{Q_a^0} \dot{\mathbf{q}} + \frac{Q_b^0}{\exp(k_b q_0^b / Q_b^0)} \mathbf{K}^s, \tag{57}$$

$$\dot{q}_0^b = \frac{k_e}{k_b Q_a^0} \mathbf{Q}_b^T \dot{\mathbf{q}} + \frac{Q_b^0 K^0}{k_b \exp(k_b q_0^b / Q_b^0)}, \tag{58}$$

where

$$\overset{\circ}{\mathbf{Q}}_a := \dot{\mathbf{Q}}_a - \mathbf{\Omega} \mathbf{Q}_a, \tag{59}$$

$$\overset{\circ}{\mathbf{Q}}_b := \dot{\mathbf{Q}}_b - \mathbf{\Omega} \mathbf{Q}_b. \tag{60}$$

In above, a surmounted circle "$\circ$" represents a certain corotational derivative with respect to the skew-symmetric spin matrix $\mathbf{\Omega}$, $\mathbf{K}^s := (K^1, K^2, \ldots, K^n)^T$ is an n-vector part of $\mathbf{K}$, and K^0 is a scalar part of $\mathbf{K}$.

2.5 Kinematic hardening rules

The models derived in Sections 2.3 and 2.4 are based on the group theory and their projective relatizations. However, they are not yet to be plasticity models. To fit the requirements of plasticity we should impose the following extra conditions:

$$\mathbf{X}_a^T \mathbf{g} \mathbf{X}_a \leq -r, \tag{61}$$

$$\dot{X}_a^0 \geq 0, \tag{62}$$

$$\left(\mathbf{X}_a^T \mathbf{g} \mathbf{X}_a + r\right) \dot{X}_a^0 = 0, \tag{63}$$

$$\dot{X}_b^0 \geq 0, \tag{64}$$

$$\dot{\mathbf{X}}_b = \mathbf{0} \text{ if } \dot{X}_a^0 = 0. \tag{65}$$

The first three equations consist of a complementary trio in the augmented space of $\mathbf{X}_a$. With the aid of Eqs. (48) and (49), the above equations lead to the following five equations in the space of $\mathbf{Q}$:

$$\|\mathbf{Q}_a\|^2 \leq (Q_a^0)^2 - \frac{r (Q_a^0)^2}{\exp(2k_a q_0^a / Q_a^0)}, \tag{66}$$

$$\dot{q}_0^a \geq 0, \tag{67}$$

$$\left[\|\mathbf{Q}_a\|^2 - (Q_a^0)^2 + \frac{r (Q_a^0)^2}{\exp(2k_a q_0^a / Q_a^0)}\right] \dot{q}_0^a = 0, \tag{68}$$

$$\dot{q}_0^b \geq 0, \tag{69}$$

$$\dot{\mathbf{Q}}^b = \mathbf{0} \text{ and } \dot{q}_0^b = 0 \text{ if } \dot{q}_0^a = 0. \tag{70}$$

In summary this model includes five material constants of Q_a^0, k_a, Q_b^0, k_b and r, and one rate-independent material function $\mathbf{K}$. For $r < 0$ the strain softening can be modeled, and for $0 < r < 1$ the strain hardening can be modeled. For these two cases the limiting values of $\|\mathbf{Q}_a\|$ are both Q_a^0, and the initial yield strengths are both $\sqrt{1-r}Q_a^0$. For $r = 0$ we have a purely kinematic hardening model without considering the isotropic hardening or softening. Accordingly, $\dot{q}_0^a$ in Eq. (55) must subject to the on-off switching criteria of plasticity:

$$\begin{aligned} &\dot{q}_0^a = \frac{k_e}{k_a Q_a^0}\mathbf{Q}_a^T\dot{\mathbf{q}} \\ &\quad \text{if} \quad \|\mathbf{Q}_a\|^2 = (Q_a^0)^2 - \frac{r(Q_a^0)^2}{\exp(2k_a q_0^a/Q_a^0)} \\ &\quad \text{and} \quad \mathbf{Q}_a^T\dot{\mathbf{q}} > 0, \end{aligned} \tag{71}$$

$$\begin{aligned} &\dot{q}_0^a = 0 \\ &\quad \text{if} \quad \|\mathbf{Q}_a\|^2 < (Q_a^0)^2 - \frac{r(Q_a^0)^2}{\exp(2k_a q_0^a/Q_a^0)} \\ &\quad \text{or} \quad \mathbf{Q}_a^T\dot{\mathbf{q}} \le 0. \end{aligned} \tag{72}$$

While $\dot{q}_0^a = 0$ presents the elastic state, $\dot{q}_0^a > 0$ corresponds to the plastic state. While the second condition in Eq. (71) is known as the straining condition, the first condition in Eq. (71) is known the yield condition. Depending on the value of r, the size of yield surface may expand, fix, or contract.

Similarly, under the condition of $\dot{q}_a^0 > 0$, $\dot{q}_0^b$ in Eq. (57) must subject to the following switching criteria:

$$\begin{aligned} &\dot{q}_0^b = \frac{k_e}{k_b Q_a^0}\mathbf{Q}_b^T\dot{\mathbf{q}} + \frac{Q_b^0 K^0}{k_b \exp(k_b q_0^b/Q_b^0)} \\ &\quad \text{if } \dot{q}_a^0 > 0 \\ &\quad \text{and } \frac{k_e}{k_b Q_a^0}\mathbf{Q}_b^T\dot{\mathbf{q}} + \frac{Q_b^0 K^0}{k_b \exp(k_b q_0^b/Q_b^0)} > 0, \end{aligned} \tag{73}$$

$$\begin{aligned} &\dot{q}_0^b = 0 \text{ if } \dot{q}_a^0 = 0 \\ &\quad \text{or } \frac{k_e}{k_b Q_a^0}\mathbf{Q}_b^T\dot{\mathbf{q}} + \frac{Q_b^0 K^0}{k_b \exp(k_b q_0^b/Q_b^0)} \le 0. \end{aligned} \tag{74}$$

The on and off phases of plasticity correspond to $\dot{q}_0^a > 0$ and $\dot{q}_0^a = 0$, respectively. By letting $\dot{q}_0^a = 0$ in the plastic phase equation (55), we simply obtain an elastic phase equation, namely,

$$\begin{aligned} &\overset{\circ}{\mathbf{Q}}_a = k_e\dot{\mathbf{q}} \\ &\quad \text{if } \|\mathbf{Q}_a\|^2 < (Q_a^0)^2 - \frac{r(Q_a^0)^2}{\exp(2k_a q_0^a/Q_a^0)} \\ &\quad \text{or } \mathbf{Q}_a^T\dot{\mathbf{q}} \le 0. \end{aligned} \tag{75}$$

By the switching criterion (74), from Eq. (57) we have

$$\begin{aligned} &\overset{\circ}{\mathbf{Q}}_b = \frac{k_e Q_b^0}{Q_a^0}\dot{\mathbf{q}} + \frac{Q_b^0}{\exp(k_b q_0^b/Q_b^0)}\mathbf{K}^s \\ &\quad \text{if } \dot{q}_0^a > 0 \\ &\quad \text{and } \frac{k_e}{k_b Q_a^0}\mathbf{Q}_b^T\dot{\mathbf{q}} + \frac{Q_b^0 K^0}{k_b \exp(k_b q_0^b/Q_b^0)} \le 0. \end{aligned} \tag{76}$$

It amounts to performing a switch between these two types of kinematic hardening rules: one with $\dot{q}_0^b > 0$ in Eq. (57) and one with $\dot{q}_0^b = 0$, which leading to the above equation.

2.6 *A model with corotational stress rate and kinematic hardening*

Combining Eqs. (52), (55), (57) and (76) we obtain the following flow model of plasticity:

$$\mathbf{Q} = \mathbf{Q}_a + \mathbf{Q}_b, \tag{77}$$

$$\overset{\circ}{\mathbf{Q}}_a + \frac{k_a\dot{q}_0^a}{Q_a^0}\mathbf{Q}_a = k_e\dot{\mathbf{q}}, \tag{78}$$

$$\overset{\circ}{\mathbf{Q}}_b + \frac{k_b\dot{q}_0^b}{Q_b^0}\mathbf{Q}_b = \frac{k_e Q_b^0}{Q_a^0}\dot{\mathbf{q}} + \frac{Q_b^0}{\exp(k_b q_0^b/Q_b^0)}\mathbf{K}^s, \tag{79}$$

$$\dot{q}_0^b = \left\langle \frac{k_e}{k_b Q_a^0}\mathbf{Q}_b^T\dot{\mathbf{q}} + \frac{Q_b^0 K^0}{k_b \exp(k_b q_0^b/Q_b^0)} \right\rangle \ge 0, \tag{80}$$

$$\|\mathbf{Q}_a\|^2 \le (Q_a^0)^2 - \frac{r(Q_a^0)^2}{\exp(2k_a q_0^a/Q_a^0)}, \tag{81}$$

$$\dot{q}_0^a \ge 0, \tag{82}$$

$$\left[\|\mathbf{Q}_a\|^2 - (Q_a^0)^2 + \frac{r(Q_a^0)^2}{\exp(2k_a q_0^a/Q_a^0)}\right]\dot{q}_0^a = 0, \tag{83}$$

$$\dot{\mathbf{Q}}_b = \mathbf{0}, \ \dot{q}_0^b = 0, \quad \text{if } \dot{q}_0^a = 0, \tag{84}$$

where $\langle x\rangle := (x + |x|)/2$ denotes the MacCauley bracket of x, and

$$\mathbf{K}^s = \mathbf{K}^s(\dot{\mathbf{q}}, \mathbf{Q}_a, \mathbf{Q}_b, q_0^a, q_0^b), \tag{85}$$

$$K^0 = K^0(\dot{\mathbf{q}}, \mathbf{Q}_a, \mathbf{Q}_b, q_0^a, q_0^b) \tag{86}$$

are two given continuous functions. Remind that Eqs. (77)-(84) to be a rate-independent model, $\mathbf{K}^s$ and K^0 should be rate-independent, that is,

$$\mathbf{K}^s(t')dt' = \mathbf{K}^s(t)dt, \tag{87}$$

$$K^0(t')dt' = K^0(t)dt, \tag{88}$$

where t and t' are two different time scales with $dt'/dt > 0$.

2.7 Non-associated flow rule

From Eqs. (52), (55) and (57) it follows that

$$\overset{\circ}{\mathbf{Q}} = \left(k_e + \frac{k_e Q_b^0}{Q_a^0}\right)\dot{\mathbf{q}} - \frac{k_a \dot{q}_0^a}{Q_a^0}\mathbf{Q}_a - \frac{k_b \dot{q}_0^b}{Q_b^0}\mathbf{Q}_b + \frac{Q_b^0}{\exp(k_b q_0^b/Q_b^0)}\mathbf{K}^s. \tag{89}$$

Now, using

$$\dot{\mathbf{q}} = \dot{\mathbf{q}}^e + \dot{\mathbf{q}}^p, \tag{90}$$

$$\overset{\circ}{\mathbf{Q}} = k_e \dot{\mathbf{q}}^e, \tag{91}$$

one obtains

$$\dot{\mathbf{q}}^p = \frac{k_a \dot{q}_0^a}{k_e Q_a^0}\mathbf{Q}_a + \frac{k_b \dot{q}_0^b}{k_e Q_b^0}\mathbf{Q}_b - \frac{Q_b^0}{Q_a^0}\dot{\mathbf{q}} - \frac{Q_b^0}{k_e \exp(k_b q_0^b/Q_b^0)}\mathbf{K}^s. \tag{92}$$

It indicates that the plastic flow is non-associated. An associated flow rule is that $\dot{\mathbf{q}}^p$ is proportional to $\mathbf{Q}_a$.

Taking the inner product of Eq. (57) with $\mathbf{Q}_b$ and using Eq. (73), we get

$$\mathbf{Q}_b^T \dot{\mathbf{Q}}_b = \left(k_b Q_b^0 - \frac{k_b}{Q_b^0}\mathbf{Q}_b^T \mathbf{Q}_b\right)\dot{q}_0^b + \frac{Q_b^0}{\exp(k_b q_0^b/Q_b^0)}\mathbf{Q}_b^T \mathbf{K}^s - \frac{(Q_a^0 Q_b^0)^2 K^0}{\exp(k_b q_0^b/Q_b^0)}. \tag{93}$$

If $\mathbf{Q}_b^T \mathbf{Q}_b = (Q_b^0)^2$ the first term on the right-hand side disappears, and thus $d\|\mathbf{Q}_b\|/dt = o(1)$ under the following condition:

$$Q_b^0 \mathbf{Q}_b^T \mathbf{K}^s - (Q_a^0 Q_b^0)^2 K^0 = o(\exp(k_b q_0^b/Q_b^0)), \tag{94}$$

where $a = o(b)$ means that $a/b \to 0$. Because $\mathbf{K}$ is bounded, and the exponential term $\exp(k_b q_0^b/Q_b^0)$ approaches to a very large value when q_0^b is large enough, the above condition is satisfied. Thus the norm of $\mathbf{Q}_b$ has a limiting value. In addition to the usual yield hypersphere this model also implies a limiting surface existent. Unlike to the two-surface theories which postulate a priori the existence of a limiting surface, the present formulation based on the group theory results directly the existence of a limiting surface, and is able to describe the nonlinearity of kinematic hardening continuously.

2.8 Symmetry switching between $SE(n)$ and $PISO_o(n,1)$

The complemantary trio may render the validity of the $ISO_o(n,1)$ symmetry to be restricted on the moving cone, when the dynamical system is in the plastic phase. In the elastic phase Eq. (55) becomes

$$\dot{\mathbf{Q}}_a = \mathbf{\Omega}\mathbf{Q}_a + k_e \dot{\mathbf{q}}, \tag{95}$$

and $\mathbf{Q}_b$ is fixed. It is clear from the previous derivation that $\mathbf{\Omega}$ belongs to the real Lie algebra $so(n)$ of the n-dimensional special orthogonal (or proper rotation) group $SO(n)$, which is the group of rotations of the n-space of $(Q^1, Q^2, \ldots, Q^n)$ around its origin $(0, 0, \ldots, 0)$. Hence, in the elastic phase we have

$$\mathbf{G} = \begin{bmatrix} \mathbf{G}_s^s & \mathbf{G}_0^s \\ \mathbf{0}_{1\times n} & 1 \end{bmatrix} \tag{96}$$

with

$$\dot{\mathbf{G}}_s^s = \mathbf{\Omega}\mathbf{G}_s^s, \tag{97}$$

$$\dot{\mathbf{G}}_0^s = \mathbf{\Omega}\mathbf{G}_0^s + \frac{1}{q_y}\dot{\mathbf{q}}. \tag{98}$$

where $\mathbf{G}_s^s \in SO(n)$, $\mathbf{G}_0^s \in T(n)$, and $\mathbf{G} \in SE(n)$, and the dynamical system has an internal symmetry characterized by the special Euclidean (or proper motion) group $SE(n)$, which is the semi-direct product of the translation group $T(n)$ with the proper rotation group $SO(n)$.

As a result the large deformation kinematic hardening model of elastoplasticity obtained in Section 2.6 has a *symmetry switching* between the special Euclidean group $SE(n)$ acting on the closed n-ball of admissible states in the state space of $\mathbf{Q}$ and the projective proper orthochronous Poincaré group $PISO_o(n,1)$ acting on the yield hypersphere.

3 Existent kinematic hardening rules

After deriving the flow model of elastoplasticity by a consideration of the Poincaré group and its projection, it is now a good position to compare our model with some existent kinematic hardening models. In the literature of plasticity a great effort was devoted to the constitutive equations of elastoplastic materials. In order to model the complex behavior of materials under a vast range of loading conditions, some different kinds of kinematic hardening models were proposed in the past, and those rules are summarized by the following equation (Liu, 1993):

$$\begin{aligned}\dot{\mathbf{Q}}_b = & -c_1\dot{q}_0^a\mathbf{Q}_b + c_2\dot{\mathbf{q}}^p + c_3\dot{q}_0^a\mathbf{q}^p \\ & + c_4\dot{\mathbf{Q}} + c_5\dot{q}_0^a\mathbf{Q},\end{aligned} \tag{99}$$

where $c_1,\ldots,c_5$ are material constants. It encompasses the following kinematic hardening rules proposed in the literature as special cases:

(i) $\dot{\mathbf{Q}}_b = c_4\dot{\mathbf{Q}}$ Melan (1938)
(ii) $\dot{\mathbf{Q}}_b = c_2\dot{\mathbf{q}}^p$ Prager (1956)
(iii) $\dot{\mathbf{Q}}_b = c_1\dot{q}_0^a(\mathbf{Q}-\mathbf{Q}_b)$ Ziegler (1959)
(iv) $\dot{\mathbf{Q}}_b = c_2\dot{\mathbf{q}}^p + c_4\dot{\mathbf{Q}}$ Phillips and Lee (1979)
(v) $\dot{\mathbf{Q}}_b = c_2\dot{\mathbf{q}}^p - c_1\dot{q}_0^a\mathbf{Q}_b$ Armstrong and Frederick (1966)
(vi) $\dot{\mathbf{Q}}_b = c_2\dot{\mathbf{q}}^p + c_3\dot{q}_0^a\mathbf{q}^p$ Mróz, Shrivastava and Dubey (1976)
(vii) $\dot{\mathbf{Q}}_b = -c_1\dot{q}_0^a\mathbf{Q}_b + c_2\dot{\mathbf{q}}^p + c_3\dot{q}_0^a\mathbf{q}^p$ Walker (1981)
(viii) $\dot{\mathbf{Q}}_b = -c_1\dot{q}_0^a\mathbf{Q}_b + c_4\dot{\mathbf{Q}} + c_5\dot{q}_0^a\mathbf{Q}$ Tseng and Lee (1983)
(ix) $\dot{\mathbf{Q}}_b = -c_1\dot{q}_0^a\mathbf{Q}_b + c_2\dot{\mathbf{q}}^p + c_4\dot{\mathbf{Q}}$ Ramaswamy, Stouffer and Laflen (1990)
(x) $\dot{\mathbf{Q}}_b = -c_1\dot{q}_0^a\mathbf{Q}_b + c_2\dot{\mathbf{q}}^p + c_5\dot{q}_0^a\mathbf{Q}$ Trampczyński and Mróz (1992)
(xi) $\dot{\mathbf{Q}}_b = -c_1\dot{q}_0^a\mathbf{Q}_b + c_2\dot{\mathbf{q}}^p + c_4\dot{\mathbf{Q}} + c_5\dot{q}_0^a\mathbf{Q}$ Freed, Chaboche and Walker (1991)
(xii) $\dot{\mathbf{Q}}_b = -c_1\dot{q}_0^a\mathbf{Q}_b + c_2\dot{\mathbf{q}}^p + c_3\dot{q}_0^a\mathbf{q}^p + c_4\dot{\mathbf{Q}} + c_5\dot{q}_0^a\mathbf{Q}$ Kurtyka and Życzkowski (1996)

An integral representation of the above kinematic hardening rules combined with the von Mises yield criterion have been derived by Liu (1993). In Table 1 we write the above kinematic hardening rules by pointing out the zeros of $c_1,\ldots,c_5$.

We should note that there exists only one intrinsic time q_0^a in the conventional plasticity theory. In order to give a comparison between the model in Section 2 with some kinematic hardening rules listed in Table 1 and also some recent modifications of the kinematic hardening rule of Armstrong and Frederick (1966), we may consider the following three types:

$$q_0^b = 0,\ \ q_0^a \neq 0,\ \ \text{type I}, \tag{100}$$

$$q_0^a = q_0^b \neq 0,\ \ \text{type II}, \tag{101}$$

$$q_0^a \neq q_0^b \neq 0,\ \ \text{type III}. \tag{102}$$

The results of the above formulations will be given below to compare with some kinematic hardening rules proposed in the literature. And for this purpose we let $\mathbf{\Omega} = \mathbf{0}$ hereafter.

3.1 *Type I models*

In this section we give a direct extension of the Prager kinematic hardening rule presented in the space of $\mathbf{X}$ and compare it with some nonlinear kinematic hardening rules in the space of $\mathbf{Q}$. In the frame of Section 2, we revisit the bilinear model as analyzed by Hong and Liu (1999b), where the non-homogeneous term $\mathbf{K}$ is found to be

$$\mathbf{K} = \begin{bmatrix} \frac{k_b\dot{q}_0^a}{(Q_a^0)^2}\mathbf{Q}_a - \frac{k_e}{Q_a^0}\dot{\mathbf{q}} \\ -\frac{k_e}{(Q_a^0)^2}\mathbf{Q}_b^T\dot{\mathbf{q}} \end{bmatrix}. \tag{103}$$

An extension of the Prager kinematic hardening rule can be made via the following assignments:

$$\mathbf{K}^s = \frac{k_b\dot{q}_0^a}{(Q_a^0)^2}\mathbf{Q}_a - \frac{k_e}{Q_a^0}\dot{\mathbf{q}} + \mathbf{K}_e^s, \tag{104}$$

$$K^0 = -\frac{k_e}{(Q_a^0)^2}\mathbf{Q}_b^T\dot{\mathbf{q}}. \tag{105}$$

We have fixed $X_b^0 = 1$ due to $q_0^b = 0$, and added one extra term $\mathbf{K}_e^s$ in Eq. (104) to extend the bilinear model specified by Eq. (103).

Substituting Eq. (104) into Eq. (79) we find that

$$\dot{\mathbf{Q}}_b = \frac{k_b\dot{q}_0^a}{Q_a^0}\mathbf{Q}_a + Q_a^0\mathbf{K}_e^s, \tag{106}$$

which can be expressed in terms of $\dot{\mathbf{q}}^p$ by using Eq. (92) with $\dot{q}_0^b = 0$,

$$\dot{\mathbf{Q}}_b = k_b\dot{\mathbf{q}}^p + \frac{k_aQ_a^0}{k_e}\mathbf{K}_e^s. \tag{107}$$

It is easy to check that in the case of bilinear model, *i.e.*, $\mathbf{K}_e^s = \mathbf{0}$, the Prager kinematic hardening rule $\dot{\mathbf{Q}}_b = k_b\dot{\mathbf{q}}_p$ is recovered.

Table 1 : Some nonlinear kinematic hardening rules

(i)	$\dot{\mathbf{Q}}_b = c_4\dot{\mathbf{Q}}$	$c_1 = c_2 = c_3 = c_5 = 0$
(ii)	$\dot{\mathbf{Q}}_b = c_2\dot{\mathbf{q}}^p$	$c_1 = c_3 = c_4 = c_5 = 0$
(iii)	$\dot{\mathbf{Q}}_b = c_1\dot{q}_0^a(\mathbf{Q}-\mathbf{Q}_b)$	$c_2 = c_3 = c_4 = 0, c_5 = c_1$
(iv)	$\dot{\mathbf{Q}}_b = c_2\dot{\mathbf{q}}^p + c_4\dot{\mathbf{Q}}$	$c_1 = c_3 = c_5 = 0$
(v)	$\dot{\mathbf{Q}}_b = c_2\dot{\mathbf{q}}^p - c_1\dot{q}_0^a\mathbf{Q}_b$	$c_3 = c_4 = c_5 = 0$
(vi)	$\dot{\mathbf{Q}}_b = c_2\dot{\mathbf{q}}^p + c_3\dot{q}_0^a\mathbf{q}^p$	$c_1 = c_4 = c_5 = 0$
(vii)	$\dot{\mathbf{Q}}_b = -c_1\dot{q}_0^a\mathbf{Q}_b + c_2\dot{\mathbf{q}}^p + c_3\dot{q}_0^a\mathbf{q}^p$	$c_4 = c_5 = 0$
(viii)	$\dot{\mathbf{Q}}_b = -c_1\dot{q}_0^a\mathbf{Q}_b + c_4\dot{\mathbf{Q}} + c_5\dot{q}_0^a\mathbf{Q}$	$c_2 = c_3 = 0$
(ix)	$\dot{\mathbf{Q}}_b = -c_1\dot{q}_0^a\mathbf{Q}_b + c_2\dot{\mathbf{q}}^p + c_4\dot{\mathbf{Q}}$	$c_3 = c_5 = 0$
(x)	$\dot{\mathbf{Q}}_b = -c_1\dot{q}_0^a\mathbf{Q}_b + c_2\dot{\mathbf{q}}^p + c_5\dot{q}_0^a\mathbf{Q}$	$c_3 = c_4 = 0$
(xi)	$\dot{\mathbf{Q}}_b = -c_1\dot{q}_0^a\mathbf{Q}_b + c_2\dot{\mathbf{q}}^p + c_4\dot{\mathbf{Q}} + c_5\dot{q}_0^a\mathbf{Q}$	$c_3 = 0$
(xii)	$\dot{\mathbf{Q}}_b = -c_1\dot{q}_0^a\mathbf{Q}_b + c_2\dot{\mathbf{q}}^p + c_3\dot{q}_0^a\mathbf{q}^p + c_4\dot{\mathbf{Q}} + c_5\dot{q}_0^a\mathbf{Q}$	$c_1,\dots,c_5 \neq 0$

Now, we let

$$Q_a^0\mathbf{K}_e^s = a_1\dot{q}_0^a\mathbf{Q}_a + a_2\dot{\mathbf{q}} + a_3\dot{\mathbf{Q}}_a + a_4\dot{q}_0^a\mathbf{q}, \tag{108}$$

where $a_1,\dots,a_4$ are material constants. Obviously, the above $\mathbf{K}^s$ and K^0 meet the requirement of rate-independence in Eqs. (87) and (88). It together with Eq. (107) generate Eq. (99) with the following $c_1,\dots,c_5$:

$$c_1 = \frac{a_1k_a}{k_e+a_3k_a}, \tag{109}$$

$$c_2 = \frac{k_ek_b+a_2k_a}{k_e+a_3k_a}, \tag{110}$$

$$c_3 = \frac{a_4k_a}{k_e+a_3k_a}, \tag{111}$$

$$c_4 = \frac{a_2k_a}{k_e(k_e+a_3k_a)} + \frac{a_3k_a}{k_e+a_3k_a}, \tag{112}$$

$$c_5 = \frac{a_4k_a}{k_e(k_e+a_3k_a)} + \frac{a_1k_a}{k_e+a_3k_a}, \tag{113}$$

where $k_a = k_e + k_b$ as mentioned is the active modulus. Of course we need $a_3 \neq -k_e/k_a$ to avoid the zero denominators. Utilizing the above information some kinematic hardening rules listed in Table 1 can be realized through type I formulation as shown in Table 2.

3.2 *Type II models*

Let

$$\exp(k_bq_0^b/Q_b^0) = \exp(k_aq_0^a/Q_a^0), \tag{114}$$

$$\mathbf{K}^s = \exp(k_aq_0^a/Q_a^0)\mathbf{K}_e^s, \tag{115}$$

$$K^0 = \frac{\exp(k_aq_0^a/Q_a^0)}{q_y}\left(\frac{\mathbf{Q}_a}{Q_a^0} - \frac{\mathbf{Q}_b}{Q_b^0}\right)^T\dot{\mathbf{q}}. \tag{116}$$

For this model one has $Q_b^0 = k_bQ_a^0/k_a$ because of $q_0^a = q_0^b$. Thus using Eqs. (90) and (91), Eq. (79) changes to

$$\dot{\mathbf{Q}}_b + \frac{k_b\dot{q}_0^a}{Q_b^0}\mathbf{Q}_b = \frac{k_eQ_b^0}{Q_a^0}\dot{\mathbf{q}}^p + \frac{Q_b^0}{Q_a^0}\dot{\mathbf{Q}} + Q_b^0\mathbf{K}_e^s. \tag{117}$$

Depending on Q_b^0, k_b and $\mathbf{K}_e^s$ the above kinematic hardening rule may be an extension of some kinematic hardening rules listed in Table 1. For the comparison purpose we let

$$Q_b^0\mathbf{K}_e^s = a_1\dot{q}_0^a\mathbf{Q}_a + a_2\dot{\mathbf{q}} + a_3\dot{\mathbf{Q}}_a + a_4\dot{q}_0^a\mathbf{q}, \tag{118}$$

where $a_1,\dots,a_4$ are material constants. The above equation together with Eq. (117) generate Eq. (99) again, but with the following $c_1,\dots,c_5$:

$$c_1 = \frac{k_b}{(1+a_3)Q_b^0} + \frac{a_1}{1+a_3}, \tag{119}$$

$$c_2 = \frac{k_eQ_b^0}{(1+a_3)Q_a^0} + \frac{a_2}{1+a_3}, \tag{120}$$

$$c_3 = \frac{a_4}{1+a_3}, \tag{121}$$

$$c_4 = \frac{Q_b^0}{(1+a_3)Q_a^0} + \frac{a_2}{k_e(1+a_3)} + \frac{a_3}{1+a_3}, \tag{122}$$

$$c_5 = \frac{a_4}{k_e(1+a_3)} + \frac{a_1}{1+a_3}. \tag{123}$$

Similarly, $\mathbf{K}^s$ and K^0 meet the requirement of rate-independence in Eqs. (87) and (88). In above, a_3 should be not equal to -1 to avoid the zero denominators. Utilizing the above information some kinematic hardening rules listed in Table 1 can be obtained through type II formulation as shown in Table 2.

Table 2 : Comparing the nonlinear kinematic hardening rules with type I and type II formulations

	Type I	Type II
(i)	$a_1 = a_4 = 0$, $a_2 = -k_e k_b/k_a$	not applicable
(ii)	$a_1 = a_2 = a_3 = a_4 = 0$	not applicable
(iii)	$a_1 = a_2 = a_3 = a_4 = 0$	not applicable
(iv)	$a_1 = a_4 = 0$	not applicable
(v)	not applicable	$a_1 = a_4 = 0$, $a_3 = -a_2/k_e - Q_b^0/Q_a^0$
(vi)	not applicable	$a_1 = -k_b/Q_b^0$, $a_3 = -a_2/k_e - Q_b^0/Q_a^0$, $a_4 = k_e k_b/Q_b^0$
(vii)	$a_2 = -k_e a_3$, $a_4 = -k_e a_1$	$a_1 = -a_4/k_e$, $a_3 = -a_2/k_e - Q_b^0/Q_a^0$
(viii)	$a_4 = 0$, $a_2 = -k_e k_b/k_a$	$a_4 = 0$, $a_2 = -k_e Q_b^0/Q_a^0$
(ix)	not applicable	$a_1 = a_4 = 0$
(x)	$a_4 = 0$, $a_2 = -k_e a_3$	$a_4 = 0$, $a_3 = -a_2/k_e - Q_b^0/Q_a^0$
(xi)	$a_4 = 0$	$a_4 = 0$
(xii)	applicable	applicable

3.3 Overlook on the kinematic hardening rules with two intrinsic times

When the characterization of q_0^b is allowed to be different from q_0^a, it leaves us a freedom to specify q_0^b independently.

3.3.1 Type IIIA models

The model derived in Section 2 is a rather general one, which leaves the form of $\mathbf{K}$ unspecified. In this section we give an example. The simplest one is obtained by letting $\mathbf{K}$ in Eq. (39) to be

$$\mathbf{K} = c_0 \mathbf{A} \mathbf{X}_a, \tag{124}$$

where c_0 is a constant. If $c_0 = 0$ an isotropic hardening model is recovered. Substituting Eqs. (28) and (48) into the above equation we obtain

$$\mathbf{K}^s = \frac{k_e c_0 \exp(k_a q_0^a/Q_a^0)}{Q_a^0} \dot{\mathbf{q}}, \tag{125}$$

$$K^0 = \frac{k_e c_0 \exp(k_a q_0^a/Q_a^0)}{(Q_a^0)^2} \mathbf{Q}_a^T \dot{\mathbf{q}}. \tag{126}$$

For this case we have the following kinematic hardening rule:

$$\begin{aligned} &\dot{\mathbf{Q}}_b + \frac{k_b \dot{q}_0^b}{Q_b^0} \mathbf{Q}_b \\ &= \frac{k_e Q_b^0}{Q_a^0} \left[1 + c_0 \exp\left(k_a q_0^a/Q_a^0 - k_b q_0^b/Q_b^0 \right) \right] \dot{\mathbf{q}}. \end{aligned} \tag{127}$$

3.3.2 Type IIIB models

Let

$$\mathbf{K}^s = \frac{\exp(k_b q_0^b/Q_b^0)}{Q_b^0} \left[a_0 \dot{\mathbf{q}} - \left(\frac{a_0}{k_e} + \frac{Q_b^0}{Q_a^0} \right) \dot{\mathbf{Q}}_a \right], \quad K^0 = 0, \tag{128}$$

where a_0 satisfying

$$a_0 < k_e \left(1 - \frac{Q_b^0}{Q_a^0} \right) < 0 \tag{129}$$

is a material constant. Thus, Eq. (79) becomes

$$\begin{aligned} \dot{\mathbf{Q}}_b + \frac{k_b \dot{q}_0^b}{Q_b^0} \mathbf{Q}_b = \left(\frac{k_e Q_b^0}{Q_a^0} + a_0 \right) \dot{\mathbf{q}} \\ - \left(\frac{a_0}{k_e} + \frac{Q_b^0}{Q_a^0} \right) \dot{\mathbf{Q}}_a, \end{aligned} \tag{130}$$

which upon using Eqs. (90), (91) and (77) further changes to

$$\dot{\mathbf{Q}}_b + c_1 \dot{q}_0^b \mathbf{Q}_b = c_2 \dot{\mathbf{q}}^p, \tag{131}$$

where

$$c_1 := \frac{k_e k_b Q_a^0}{Q_b^0 (k_e Q_a^0 - k_e Q_b^0 - a_0 Q_a^0)} > 0, \tag{132}$$

$$c_2 := \frac{k_e Q_a^0 a_0 + k_e^2 Q_b^0}{k_e Q_a^0 - k_e Q_b^0 - a_0 Q_a^0} > 0 \tag{133}$$

are material constants.

Eq. (131) is an extension of the famous kinematic hardening rule proposed by Armstrong and Frederick (1966), but in the present model the dynamic recovery term is controlled by $\dot{q}_0^b$ rather than that by $\dot{q}_0^a$ as the usual one. The dynamic recovery term is not always working even in the plastic loading state, the criterion of which, by Eq. (80) and $K^0 = 0$, is

$$\dot{q}_0^b = \frac{k_e}{k_b Q_a^0} \left\langle \mathbf{Q}_b^T \dot{\mathbf{q}} \right\rangle. \tag{134}$$

Figure 4 gives a schematical plot in the two-dimensional stress space of (Q^1, Q^2) to describe the evolution of back stress under two consequential proportional paths. Depending on the loading history there exist three possibilities:

$\dot{q}_0^a = \dot{q}_0^b = 0$ segments OA and BC,

$\dot{q}_0^a > 0,\ \dot{q}_0^b > 0$ segments AB and DE,

$\dot{q}_0^a > 0,\ \dot{q}_0^b = 0$ segment CD.

In the case of $\mathbf{Q}_b^T \dot{\mathbf{q}} < 0$ the dynamic recovery term is turned-off even in the plastic phase.

The above formulation provides a very natural and useful modification of the kinematic hardening rule of Armstrong and Frederick. In this occasion we should also mention the modifications proposed by Chaboche (1991) and Ohno and Wang (1993). In their modifications the back stress is divided into several subparts, *i.e.*,

$$\mathbf{Q}_b = \sum_{i=1}^{m} \mathbf{Q}_b^i, \tag{135}$$

and each $\mathbf{Q}_b^i$ obeys the following rules:

$$\dot{\mathbf{Q}}_b^i + a_i \langle \|\mathbf{Q}_b^i\| - b_i \rangle^{m_i} \dot{q}_0^a \frac{\mathbf{Q}_b^i}{\|\mathbf{Q}_b^i\|} = b_i \dot{\mathbf{q}}^p, \quad \text{Chaboche (1991)}, \tag{136}$$

$$\dot{\mathbf{Q}}_b^i + a_i H(\|\mathbf{Q}_b^i\| - b_i) \langle (\mathbf{Q}_b^i)^T \mathbf{n} \rangle \dot{q}_0^a \frac{\mathbf{Q}_b^i}{\|\mathbf{Q}_b^i\|} = b_i \dot{\mathbf{q}}^p, \quad \text{Ohno and Wang (1993)}. \tag{137}$$

The above a_i, b_i, c_i and m_i are material constants; b_i is a threshold value of $\|\mathbf{Q}_b^i\|$, H is the Heaviside step function, and $\mathbf{n}$ is the plastic strain rate direction. It should note that both rules include only one intrinsic time q_0^a, and the practical applications require the superposition of a fairly large number of independent sub-back stresses; see, for example, the comments by Chaboche (1994).

Both rules use a critical state of the dynamic recovery term to improve the simulation of ratcheting behavior. If we let

$$\dot{q}_0^b := \frac{\langle \|\mathbf{Q}_b^i\| - b_i \rangle^{m_i}}{\|\mathbf{Q}_b^i\|} \dot{q}_0^a, \quad \text{Chaboche (1991)}, \tag{138}$$

$$\dot{q}_0^b := H(\|\mathbf{Q}_b^i\| - b_i) \frac{\langle (\mathbf{Q}_b^i)^T \mathbf{n} \rangle}{\|\mathbf{Q}_b^i\|} \dot{q}_0^a, \quad \text{Ohno and Wang (1993)}, \tag{139}$$

the kinematic hardening rules obtained are similar to Eq. (131) when applied it to the sub-back stress $\mathbf{Q}_b^i$; however, according to the above definitions q_0^b is not independent to q_0^a. For a typical loading history there also exist three possibilities:

$$\dot{q}_0^a = \dot{q}_0^b = 0, \tag{140}$$

$$\dot{q}_0^a > 0,\ \dot{q}_0^b > 0, \tag{141}$$

$$\dot{q}_0^a > 0,\ \dot{q}_0^b = 0. \tag{142}$$

The main difference between the present model with those of Chaboche (1991) and Ohno and Wang (1993) is that our model exhibits two independent intrinsic times rather than the usual one intrinsic time formulation. Comparisons between the present model with the ones of Chaboche (1991) and Ohno and Wang (1993) are summarized in Table 3. Recent progress of the Ohno-Wang model and its numerical computation are discussed by Chen, Jiao and Kim (2005) and Abdel-Karim (2005).

4 Numerical computations

For calculation purpose we may approximate the specified controlled-strain path by many rectilinear strain paths, such that $\dot{\mathbf{q}}(t)$ at each time step is constant. We first consider elastic phase. Under a specified strain path of $\mathbf{q}(t)$ and initial stresses of $\mathbf{Q}_a(t_i)$ and $\mathbf{Q}_b(t_i)$ and a fixed $q_0^a(t_i)$, the elastic responses can be obtained by

$$\mathbf{Q}_a(t) = \mathbf{Q}_a(t_i) + k_e[\mathbf{q}(t) - \mathbf{q}(t_i)], \tag{143}$$

$$\mathbf{Q}(t) = \mathbf{Q}_a(t) + \mathbf{Q}_b(t_i), \tag{144}$$

since the back stress is fixed to be $\mathbf{Q}_b(t_i)$. The end time of elastic phase denoted by t_{on} can be determined according to the criterion (71) as follows. First solve for t the

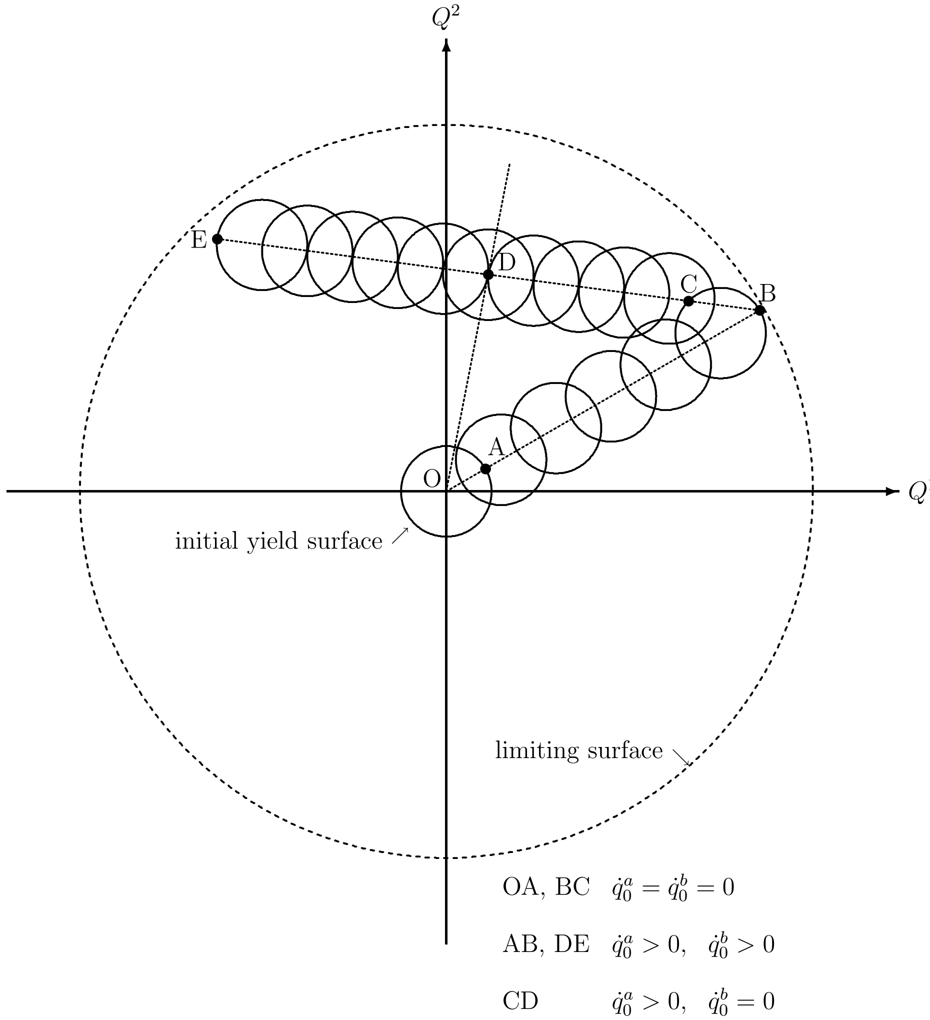

Figure 4 : Based on the kinematic hardening rule derived from the Poincaré group theory the evolution of back stress in the space of (Q^1, Q^2) is described for two sequential rectilinear strain paths. This model includes two intrinsic times q_0^a and q_0^b. In the segment CD the dynamic recovery term in the back stress equation is switched off, *i.e.* $\dot{q}_0^b = 0$.

following algebraic equation

$$\begin{aligned} &\|\mathbf{Q}_a(t_i)\|^2 + 2k_e[\mathbf{q}(t) - \mathbf{q}(t_i)]^T \mathbf{Q}_a(t_i) \\ &\quad + k_e^2 \|\mathbf{q}(t) - \mathbf{q}(t_i)\|^2 \\ &\quad = (Q_a^0)^2 - \frac{r(Q_a^0)^2}{\exp(2k_a q_0^a(t_i)/Q_a^0)}, \end{aligned} \tag{145}$$

which has been obtained by substituting the elastic equation (143) into the yield condition $\|\mathbf{Q}_a\|^2 = (Q_a^0)^2 - r(Q_a^0)^2/\exp(2k_a q_0^a/Q_a^0)$.

However, the solution t of Eq. (145) must satisfy $\mathbf{Q}_a^T(t)\dot{\mathbf{q}}(t) > 0$ in order to be a switch-on time t_{on}. If there exists no solution to Eq. (145) or the solution t to Eq. (145) doesn't satisfy $\mathbf{Q}_a^T(t)\dot{\mathbf{q}}(t) > 0$, then the strain path will not switch on the plastic mechanism.

Below we concentrate on the plastic phase with $\dot{q}_0^a > 0$. In view of Eqs. (50)-(52), calculating $\mathbf{X}_a$ and $\mathbf{X}_b$ is sufficient to obtain the responses of $\mathbf{Q}$, and we don't need the numerical solutions of Eqs. (77)-(86). Because $\mathbf{A}$ as shown in Eq. (28) is time-dependent, the closed-form solutions of $\mathbf{X}_a$ and $\mathbf{X}_b$ obtained by solving Eqs. (36) and (37) are usually not available.

Denote by I_{on} an open, maximal, continuous time interval during which the mechanism of plasticity is on exclusively. The solution of the augmented active stress equation (36) with its $\mathbf{A}$ defined in Eq. (28) with $\mathbf{\Omega} = \mathbf{0}$ can be expressed in the following augmented active stress

Table 3 : The modifications of the kinematic hardening rule of Armstrong and Frederick

	present model	Chaboche (1991)	Ohno and Wang (1993)
limiting of $\mathbf{Q}_b$	yes	yes	yes
threshold of $\|\mathbf{Q}_b^i\|$	no	$\|\mathbf{Q}_b^i\| = b_i$	$\|\mathbf{Q}_b^i\| = b_i$
intrinsic times	q_0^a, q_0^b	q_0^a, $\dot{q}_0^b = \frac{\langle \|\mathbf{Q}_b^i\| - b_i \rangle^{m_i}}{\|\mathbf{Q}_b^i\|} \dot{q}_0^a$	q_0^a, $\dot{q}_0^b = H(\|\mathbf{Q}_b^i\| - b_i) \frac{\langle \mathbf{Q}_b^{iT} \mathbf{n} \rangle}{\|\mathbf{Q}_b^i\|} \dot{q}_0^a$
three possible values of intrinsic times' rates $\dot{q}_0^a$ and $\dot{q}_0^b$	$\dot{q}_0^a = \dot{q}_0^b = 0$ $\dot{q}_0^a > 0, \dot{q}_0^b > 0$ $\dot{q}_0^a > 0, \dot{q}_0^b = 0$	$\dot{q}_0^a = \dot{q}_0^b = 0$ $\dot{q}_0^a > 0, \dot{q}_0^b > 0$ $\dot{q}_0^a > 0, \dot{q}_0^b = 0$	$\dot{q}_0^a = \dot{q}_0^b = 0$ $\dot{q}_0^a > 0, \dot{q}_0^b > 0$ $\dot{q}_0^a > 0, \dot{q}_0^b = 0$
switch of recovery term	$\mathbf{Q}_b^T \dot{\mathbf{q}} > 0$	$\|\mathbf{Q}_b^i\| = b_i$	$\|\mathbf{Q}_b^i\| = b_i$ and $(\mathbf{Q}_b^i)^T \dot{\mathbf{q}}^p > 0$
constancy of $\|\mathbf{Q}_b^i\|$	no	no	$\|\mathbf{Q}_b^i\| = b_i$ after switching

transition formula:

$$\mathbf{X}_a(t) = \mathbf{G}(t)\mathbf{G}^{-1}(t_i)\mathbf{X}_a(t_i), \quad \forall\, t, t_i \in \mathrm{I_{on}}, \tag{146}$$

in which $\mathbf{G}(t)$, known as the fundamental solution of Eq. (36), is a transformation matrix satisfying

$$\dot{\mathbf{G}}(t) = \mathbf{A}(t)\mathbf{G}(t), \tag{147}$$

$$\mathbf{G}(0) = \mathbf{I}_{n+1}. \tag{148}$$

At the same time the solution of the augmented back stress equation (37) with the same $\mathbf{A}$ can be expressed in the following augmented back stress transition formula:

$$\begin{aligned} \mathbf{X}_b(t) &= \mathbf{G}(t)\mathbf{G}^{-1}(t_i)\mathbf{X}_b(t_i) \\ &+ \int_{t_i}^{t} \mathbf{G}(t)\mathbf{G}^{-1}(\xi)\mathbf{K}(\xi)d\xi, \quad \forall\, t, t_i \in \mathrm{I_{on}}. \end{aligned} \tag{149}$$

Consider a rectilinear strain path

$$\mathbf{q}(t) = \mathbf{q}(t_i) + (t - t_i)\dot{\mathbf{q}} \tag{150}$$

with a nonzero constant rate

$$\dot{\mathbf{q}} = \text{constant} \neq \mathbf{0}, \tag{151}$$

starting from $\mathbf{q}(t_i)$ at time t_i. The constitutive response can be determined exactly (Hong and Liu, 2000), and it may be recast in the form of Eq. (146) with the augmented active stress transition matrix for the plastic phase being

$$\mathbf{G}(t)\mathbf{G}^{-1}(t_i) = \begin{bmatrix} \mathbf{I}_n + \frac{a-1}{\|\dot{\mathbf{q}}\|^2}\dot{\mathbf{q}}\dot{\mathbf{q}}^T & \frac{b\dot{\mathbf{q}}}{\|\dot{\mathbf{q}}\|} \\ \frac{b\dot{\mathbf{q}}^T}{\|\dot{\mathbf{q}}\|} & a \end{bmatrix}, \tag{152}$$

where

$$\begin{aligned} a &:= \cosh[(t - t_i)\|\dot{\mathbf{q}}\|/q_y], \\ b &:= \sinh[(t - t_i)\|\dot{\mathbf{q}}\|/q_y]. \end{aligned} \tag{153}$$

Now let us consider a general path of strain and find the responses of the considered models. To devise the numerical schemes for a time-stepping integration, let us denote the time increment by Δt and develop a mapping to update $\mathbf{Q}(t)$ to $\mathbf{Q}(t+\Delta t)$ at the next time step.

We may approximate a general strain path by a piecewise rectilinear strain path. Referring to Eq. (152), we obtain the desired mapping

$$\mathbf{G}(t+\Delta t)\mathbf{G}^{-1}(t) = \begin{bmatrix} \mathbf{I}_n + \frac{a-1}{\|\dot{\mathbf{q}}\|^2}\dot{\mathbf{q}}\dot{\mathbf{q}}^T & \frac{b\dot{\mathbf{q}}}{\|\dot{\mathbf{q}}\|} \\ \frac{b\dot{\mathbf{q}}^T}{\|\dot{\mathbf{q}}\|} & a \end{bmatrix} \tag{154}$$

with

$$a := \cosh(\Delta t\|\dot{\mathbf{q}}\|/q_y), \quad b := \sinh(\Delta t\|\dot{\mathbf{q}}\|/q_y). \tag{155}$$

For the non-homogeneous equation (37) we can apply the trapezoidal quadrature to the integral in Eq. (149) to obtain

$$\begin{aligned} \mathbf{X}_b(t+\Delta t) &= \mathbf{G}(t+\Delta t)\mathbf{G}^{-1}(t)\mathbf{X}_b(t) \\ &+ \frac{\Delta t}{2}\Big[\mathbf{K}(t+\Delta t) + \mathbf{G}(t+\Delta t)\mathbf{G}^{-1}(t)\mathbf{K}(t)\Big]. \end{aligned} \tag{156}$$

Thus a numerical scheme for the plastic phase may be devised as follows. For each time increment we first calculate the mapping (154), then update the augmented active stress vector by

$$\mathbf{X}_a(t+\Delta t) = \mathbf{G}(t+\Delta t)\mathbf{G}^{-1}(t)\mathbf{X}_a(t), \tag{157}$$

and then calculate the active stress vector $\mathbf{Q}_a(t+\Delta t)$ via Eq. (50). Second, use the mapping (154) to update the augmented back stress vector by Eq. (156), and then calculate the back stress vector $\mathbf{Q}_b(t+\Delta t)$ via Eq. (51). Finally, summing $\mathbf{Q}_a(t+\Delta t)$ and $\mathbf{Q}_b(t+\Delta t)$

we can obatin the next time response of $\mathbf{Q}(t+\Delta t)$. This algorithm automatically satisfies the yield condition at each time step without needing of iteration.

5 A smoothing technique

According to the model of type IIIB we give the stress responses as shown in Fig. 5(a) under a constant amplitude of strain input. The material constants used were $k_e = 40000$ MPa, $k_b = 5000$ MPa, $Q_a^0 = 200$ MPa, $Q_b^0 = 30$ MPa, $c_0 = 0.2$, and $r = 0.75$. From Fig. 5(a) it can be seen that the stress-strain curve is too over-square at the elastic-plastic transition points, and hence is not consistent with the usual axial tension-compression experimental testing results of metals. The reason for the above defect is that the curve of $\|\mathbf{Q}_a\|$ vs. q_0^a as shown in Fig. 5(b) is not smooth enough at the elastic-plastic transition points, while $\dot{q}_0^a$ jumps from zero values to finite values as shown in Fig. 5(c).

The yield surface

$$\|\mathbf{Q}_a\|^2 = (Q_a^0)^2\left[1 - r\exp\left(-2k_a q_0^a/Q_a^0\right)\right] \tag{158}$$

is an invariant set in the space of $(\|\mathbf{Q}_a\|, q_0^a)$. Taking the inner product of Eq. (55) with $\mathbf{Q}_a$ and using Eq. (71) lead to

$$\frac{d\|\mathbf{Q}_a\|^2}{dt} = 2k_e\mathbf{Q}_a^T\dot{\mathbf{q}}\left(1 - \frac{\|\mathbf{Q}_a\|^2}{(Q_a^0)^2}\right). \tag{159}$$

A set S in $\mathbb{R}^{n+1}$ is said to be an *invariant set* of Eq. (55) if, for any point $\mathbf{p} \in S$ the solution curve passing through $\mathbf{p}$ belongs to S for t in $(-\infty, \infty)$. In view of Eq. (159) it is obvious that

$$\begin{aligned} S := \{(\mathbf{Q}_a, q_0^a) \mid \|\mathbf{Q}_a\|^2 \\ = (Q_a^0)^2\left[1 - r\exp\left(-2k_a q_0^a/Q_a^0\right)\right]\} \end{aligned} \tag{160}$$

is an invariant set of Eq. (55). By Eq. (159) there are three disconnected sets:

$$\|\mathbf{Q}_a(t)\|^2 < (Q_a^0)^2\left[1 - r\exp\left(-2k_a q_0^a(t)/Q_a^0\right)\right], \tag{161}$$

$$\|\mathbf{Q}_a(t)\|^2 = (Q_a^0)^2\left[1 - r\exp\left(-2k_a q_0^a(t)/Q_a^0\right)\right], \tag{162}$$

$$\|\mathbf{Q}_a(t)\|^2 > (Q_a^0)^2\left[1 - r\exp\left(-2k_a q_0^a(t)/Q_a^0\right)\right]. \tag{163}$$

The state specified by Eq. (158) is the ω-limit set for arbitrary initial conditions under the condition $\mathbf{Q}_a^T\dot{\mathbf{q}} > 0$, and the α-limit set for arbitrary initial conditions under the condition $\mathbf{Q}_a^T\dot{\mathbf{q}} < 0$. Due to this characteristic of the yield surface in the conventional plasticity theory, it is not supprised that the curve of $\|\mathbf{Q}_a(t)\|$ vs. q_0^a is not smooth at the transition points as shown in Fig. 5(b). This in turn leads to the non-smoothness of Q_a^1 vs. q_1, Q_b^1 vs. q_1 as well as Q^1 vs. q_1 as shown in Fig. 5(a).

In order to circumvent the above deficiency of non-smoothness we propose a piecewise-constant yield stress as follows for rectilinear strain path (Liu, 2003b):

$$\begin{aligned} (Q_a^m)^2 &:= \|\mathbf{Q}_a(\mathrm{t_{off}})\|^2 \\ &- \frac{\rho^2B^2 - \left[(\rho-1)B + \sqrt{B^2-4AC}\right]^2}{4\rho^2A}, \end{aligned} \tag{164}$$

where

$$A := k_e^2\|\dot{\mathbf{q}}\|^2, \quad B := 2k_e\mathbf{Q}_a^T(\mathrm{t_{off}})\dot{\mathbf{q}}, \tag{165}$$

$$\begin{aligned} C &:= \|\mathbf{Q}_a(\mathrm{t_{off}})\|^2 \\ &- (Q_a^0)^2\left[1 - r\exp\left(\frac{-2k_a q_0^a(\mathrm{t_{off}})}{Q_a^0}\right)\right]. \end{aligned} \tag{166}$$

In above, $\mathrm{t_{off}}$ is the latest unloading (switching-off) time and we can let $\mathrm{t_{off}} = 0$ initially. $\rho > 1$ is a smoothing factor; when $\rho = 1$, $(Q_a^m)^2 = (Q_a^0)^2\left[1 - r\exp\left(-2k_a q_0^a(\mathrm{t_{off}})/Q_a^0\right)\right]$, and we return to the original non-smooth models. Through this modification it can be seen that $\dot{q}_0^a$ is varying smoothly from the zero value in the elastic phase to the positive value in the plastic phase as shown in Fig. 5(d), while, comparing it with Fig. 5(c), the original model leads to the jumps of $\dot{q}_0^a = 0$ in the elastic phase to finite values of $\dot{q}_0^a$ in the plastic phase. Thus, the stress-strain curves obtained by the integrations of Eqs. (55), (57) or (76) are non smooth as shown in Fig. 5(a). For the smoothing model of type IIIB with $\rho = 2$ the stress-strain curves are shown in Fig. 5(e), which are more smooth than that plotted in Fig. 5(a). The curve of $\|\mathbf{Q}_a\|$ vs. q_0^a is shown in Fig. 5(f), which reveals that the transitions from elasticity to plasticity are more smooth. The thick black curves in Figs. 5(b) and 5(f) are the invariant curves.

The specification of Q_a^m to be a new yield stress is equivalent to shorten the switching-on time by

$$\mathrm{t_{on}} = \mathrm{t_{off}} + \frac{-B + \sqrt{B^2-4AC}}{2\rho A}. \tag{167}$$

This equation is the solution of the following equation for t:

$$A(t-\mathrm{t_{off}})^2 + B(t-\mathrm{t_{off}}) + \|\mathbf{Q}_a(\mathrm{t_{off}})\|^2 - (Q_a^m)^2 = 0, \tag{168}$$

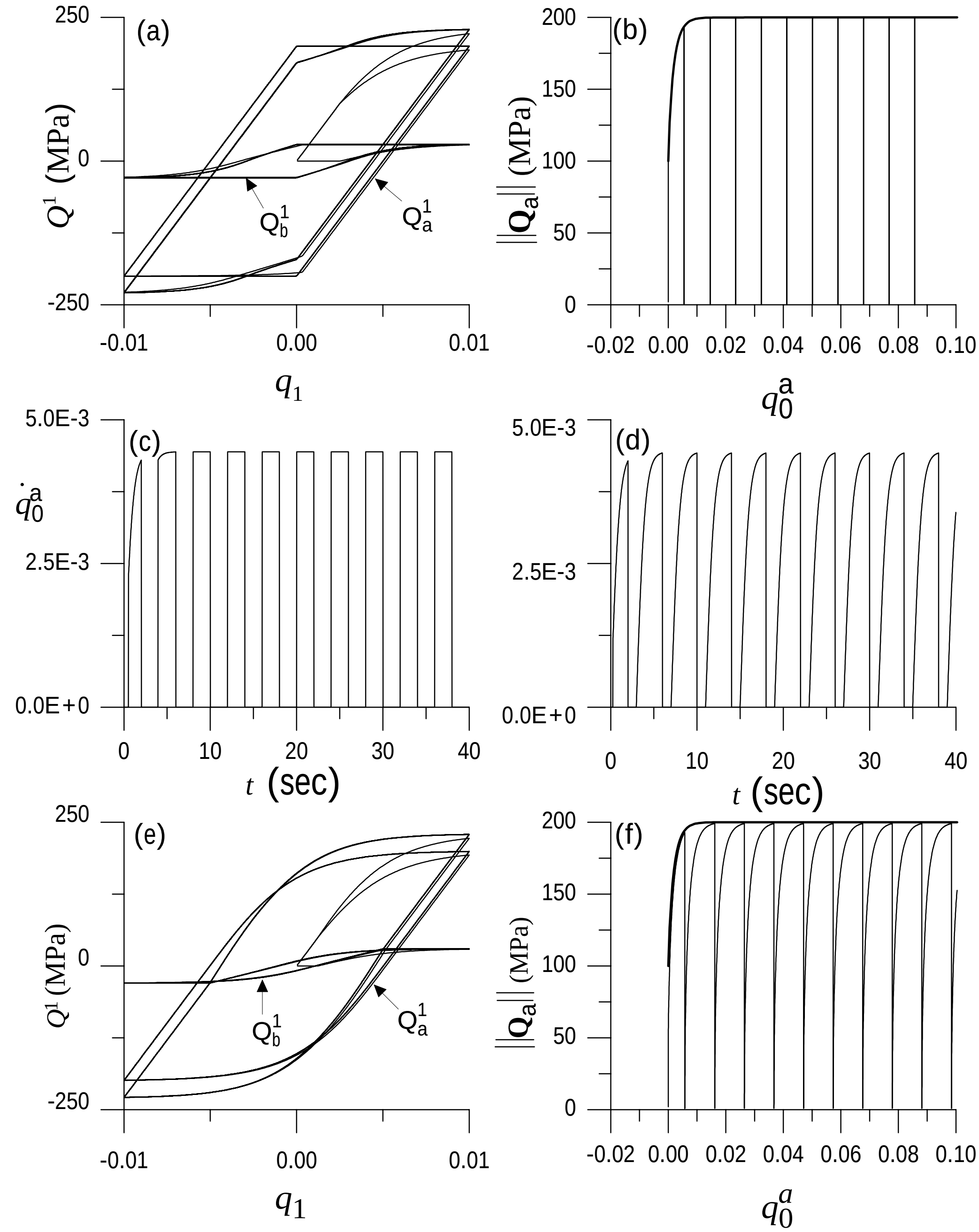

Figure 5 : For type IIIB model we compare the responses of the one without smoothing and the one with smoothing technique.

which is obtained by substituting the elastic constitutive equation $\mathbf{Q}_a(t) = \mathbf{Q}_a(t_{\text{off}}) + k_e\dot{\mathbf{q}}(t - t_{\text{off}})$ into the new yield condition $\|\mathbf{Q}_a(t)\|^2 = (Q_a^m)^2$. From Eq. (164) it can be seen that Q_a^m has a memory of the last reversal active stress point $\mathbf{Q}_a(t_{\text{off}})$. In Fig. 6 we show a stress-strain curve with $\rho = 1.5$. The monotonic loading curve is the boundary of all other unloading-reloading curve, and in the plane of $(q_0^a, \|\mathbf{Q}_a\|)$ it is an invariant curve as demonstrated above and shown in Fig. 6(b). The unloading-reloading curve will eventually approach to the monotonic loading curve if there has enough loading time; see Fig. 6(a).

In order to further understand the behaviors of the smoothing models we first subject these models to the one-dimensional shear loadings with the shear strains given in Figs. 7(a), 7(b) and 7(c), and then to the two-dimensional loadings with the strains given in Figs. 8(a), 8(b) and 8(c). The material constants used were listed in Table 4 and we fixed the smoothing factor to be $\rho = 2$. Corresponding to the four types as discussed in Section 3, we have displayed the four hysteretic curves in Fig. 7 for each shear loading case. Similarly, we have displayed the four stress paths in the plane (Q^1, Q^2) in Fig. 8 for each loading case. Under the strain loading in Fig. 8(b), the corresponding hysteretic curves of Q^1 vs. q_1 and Q^2 vs. q_2 were plotted in Fig. 9. At the same time, the hysteretic curves of Q^1 vs. q_1 and Q^2 vs. q_2 corresponding to the loading in Fig. 8(c) were plotted in Fig. 10.

Finally, we display the one-dimensional hysteretic curves under the shear loading in Fig. 11(a). For each admissible kinematic hardening model of type I and type II the material constants were summarized in Table 5. The smoothing factor is also fixed to be $\rho = 2$. In Fig. 11(j) we use $r = -0.1$, which leads to the cyclic softening of stress-strain curve.

6 Concluding remarks

This paper was starting from the Poincaré group acting on the Minkowski space. Through the construction of a Lie algebra we were able to derive three differential equations systems (35)-(37) in the augmented state spaces. The *general solution* $\mathbf{X} = \mathbf{X}_a + \mathbf{X}_b$ of Eq. (35) is the sum of the *complementary solution* $\mathbf{X}_a$ of Eq. (36) and the *particular solution* $\mathbf{X}_b$ of Eq. (37).

Upon projecting the model in the space of $(\mathbf{X}, \mathbf{X}_a, \mathbf{X}_b)$ into the model in the stresses and intrinsic times space of $(\mathbf{Q}, \mathbf{Q}_a, \mathbf{Q}_b, q_0^a, q_0^b)$ we have derived a flow theory of plasticity with large deformation and kinematic hardening by leaving the translation term $\mathbf{K}$ specified free but subject to a rate-independent requirement. The resultant models possess two intrinsic times q_0^a and q_0^b with the constraints of $\dot{q}_0^a \geq 0$ and $\dot{q}_0^b \geq 0$; the first q_0^a controls the switch of plasticity with $\dot{q}_0^a = 0$ in the elastic phase and $\dot{q}_0^a > 0$ in the plastic phase, and the second q_0^b controls the pace of back stress during the plastic phase with $\dot{q}_0^b = 0$ for the kinematic hardening rule without considering the recovery term and $\dot{q}_0^b > 0$ for the kinematic hardening rule with a recovery term.

Corresponding respectively to $q_0^b = 0$, $q_0^b = q_0^a$ and $q_0^b \neq q_0^a$ the kinematic hardening rules including the modifications of the Armstrong-Frederick kinematic hardening rule, can be classified into three types: type I, type II and type III. Combining with the smoothing technique introduced by Liu (2003b) we have modified the three types models by considering a smoothing factor. The numerical computations of the models responses were derived and some examples were plotted to show the cyclic behaviors of newly proposed models. Since the numerical method is based on the Poincaré group properties, it retains the yield condition automatically.

Acknowledgement: The financial support provided by the National Science Council of Taiwan under the Grant NSC 89-2218-E-019-020 is gratefully acknowledged.

References

Abdel-Karim, M. (2005): Numerical integration method for kinematic hardening rules with partial activation of dynamic recovery term. *Int. J. Plasticity*, vol. 21, pp. 1303-1321.

Atluri, S. N. (1984): On constitutive relations at finite strain: hypo-elasticity and elasto-plasticity with isotropic or kinematic hardening. *Comp. Meth. Appl. Mech. Eng.*, vol. 43, pp. 137-171.

Armstrong, P. J.; Frederick, C. O. (1966): A mathematical representation of the multiaxial Bauschinger effect. G.E.G.B. Report RD/B/N 731.

Chaboche, J. L. (1977): Viscoplastic constitutive equations for the description of cyclic and anisotropic behavior of solids. *Bull. l'Acad. Polish Sci., Series Sci. Tech.*,

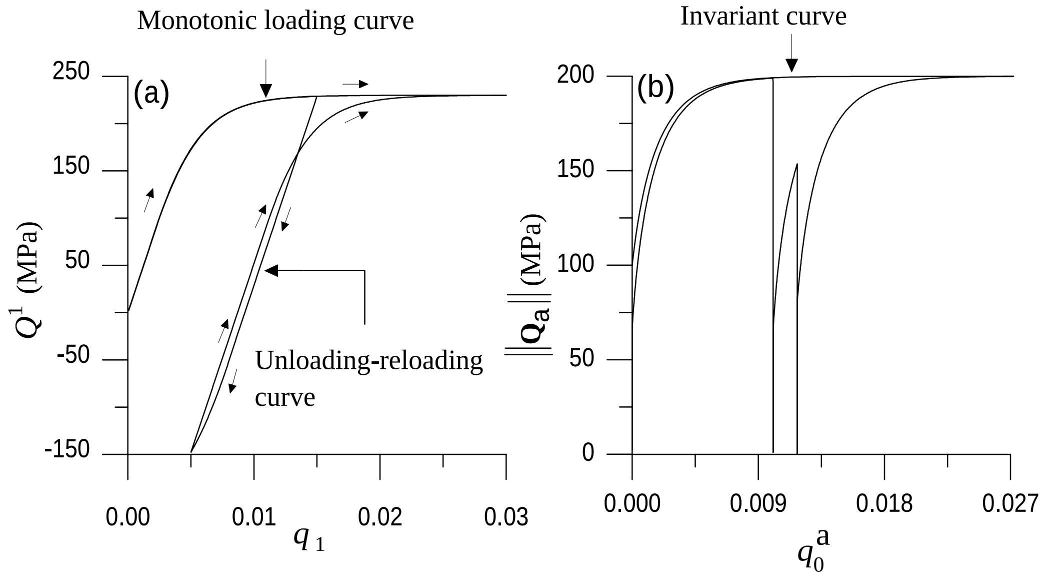

Figure 6 : For a smoothing type IIIB model we show its response curves and invariant curve.

Table 4 : The material constants used in Figures 7-10

	k_e	k_b	Q_a^0	Q_b^0	r	a_1	a_2	a_3	a_4	c_0	a_0
Type I	40000	5000	200	10	0.75	0	100	0	10	×	×
Type II	40000	10000	200	40	0.75	0	0	-0.05	0	×	×
Type IIIA	40000	×	200	10	0.75	×	×	×	×	0.2	×
Type IIIB	40000	5000	200	10	0.75	×	×	×	×	×	5000

vol. 25, pp. 33-42.

Chaboche, J. L. (1986): Time-independent constitutive theories for cyclic plasticity. *Int. J. Plasticity*, vol. 2, pp. 149-188.

Chaboche, J. L. (1989): Constitutive equations for cyclic plasticity and cyclic viscoplasticity. *Int. J. Plasticity*, vol. 5, pp. 247-302.

Chaboche, J. L. (1991): On some modifications of kinematic hardening to improve the description of ratchetting effects. *Int. J. Plasticity*, vol. 7, pp. 661-678.

Chaboche, J. L. (1993): Cyclic viscoplastic constitutive equations, part I: a thermodynamically consistent formulation, part II: stored energy. *J. Appl. Mech. ASME*, vol. 60, pp. 813-828.

Chaboche, J. L. (1994): Modeling of ratchetting: evaluation of various approaches. *Eur. J. Mech. A/Solids*, vol. 13, pp. 501-518.

Chaboche, J. L.; Cailletaud, G. (1996): Integration methods for complex plastic constitutive equations. *Comp. Meth. Appl. Mech. Eng.*, vol. 133, pp. 125-155.

Chen, X., Jiao, R., Kim, K. S. (2005): On the Ohno-Wang kinematic hardening rules for multiaxial ratcheting modeling of medium carbon steel. *Int. J. Plasticity*, vol. 21, pp. 161-184.

Eisenberg, M. A.; Phillips, A. (1968): On nonlinear kinematic hardening. *Acta Mech.*, vol. 5, pp. 1-13.

Freed, A. D.; Chaboche, J. L.; Walker, K. P. (1991): On the thermodynamics of stress rate in the evolution of back stress in viscoplasticity. *Anisotropy and Localization of Plasticity Deformation*, Proceedings of the third international symposium on plasticity and its current applications, Boehler, J.P., Khan, A.S. eds., 531-535, Elsevier, New York.

Hong, H.-K.; Liu, C.-S. (1997): Prandtl-Reuss elastoplasticity: on-off switch and superposition formulae. *Int. J. Solids Struct.*, vol. 34, pp. 4281-4304.

Hong, H.-K.; Liu, C.-S. (1998): On behavior of perfect elastoplasticity under rectilinear paths. *Int. J. Solids Struct.*, vol. 35, pp. 3539-3571.

Hong, H.-K.; Liu, C.-S. (1999a): Lorentz group

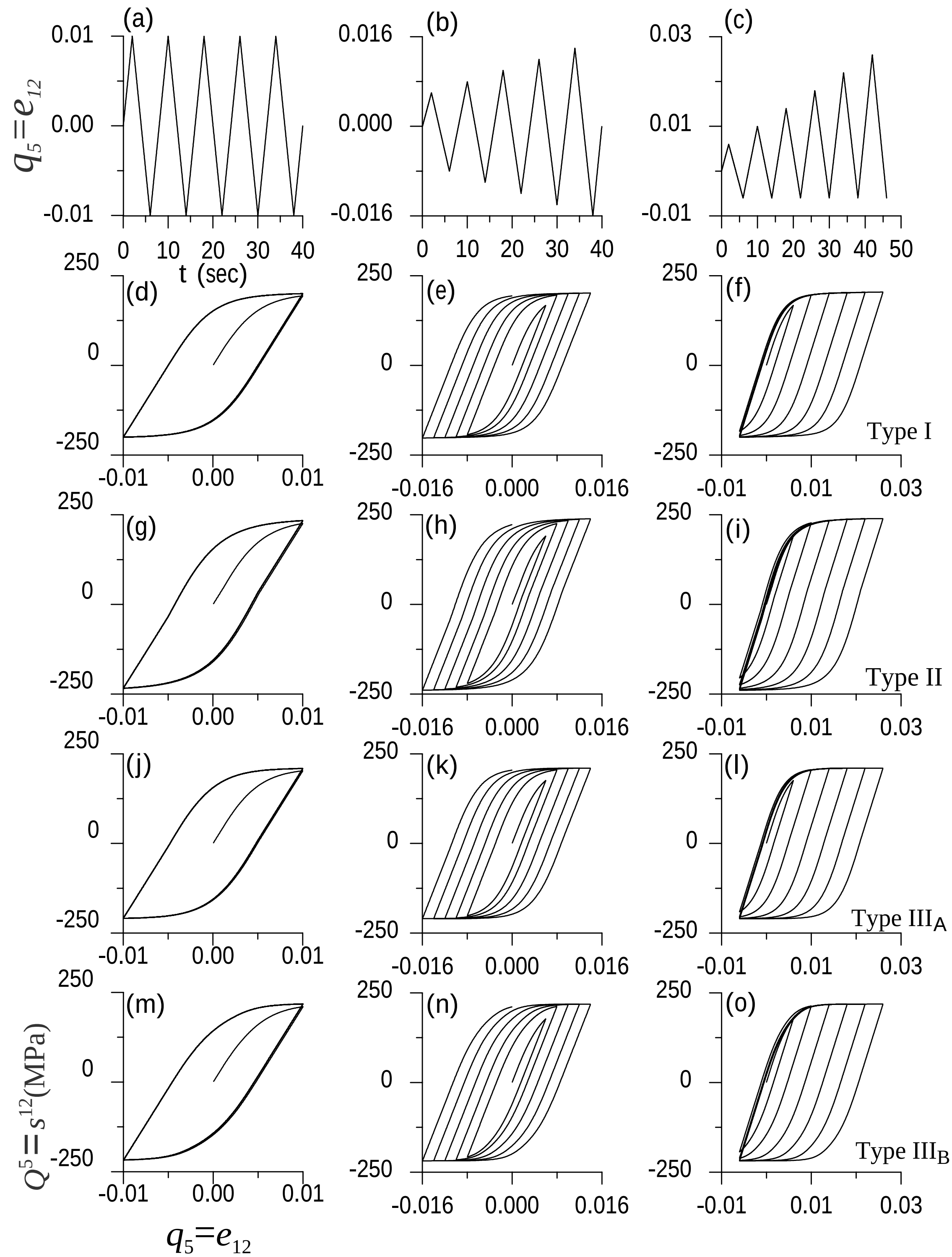

Figure 7 : Under different one-dimensional shear loading histories the hysteretic curves were shown for the smoothing type I, type II, type IIIA and type IIIB models.

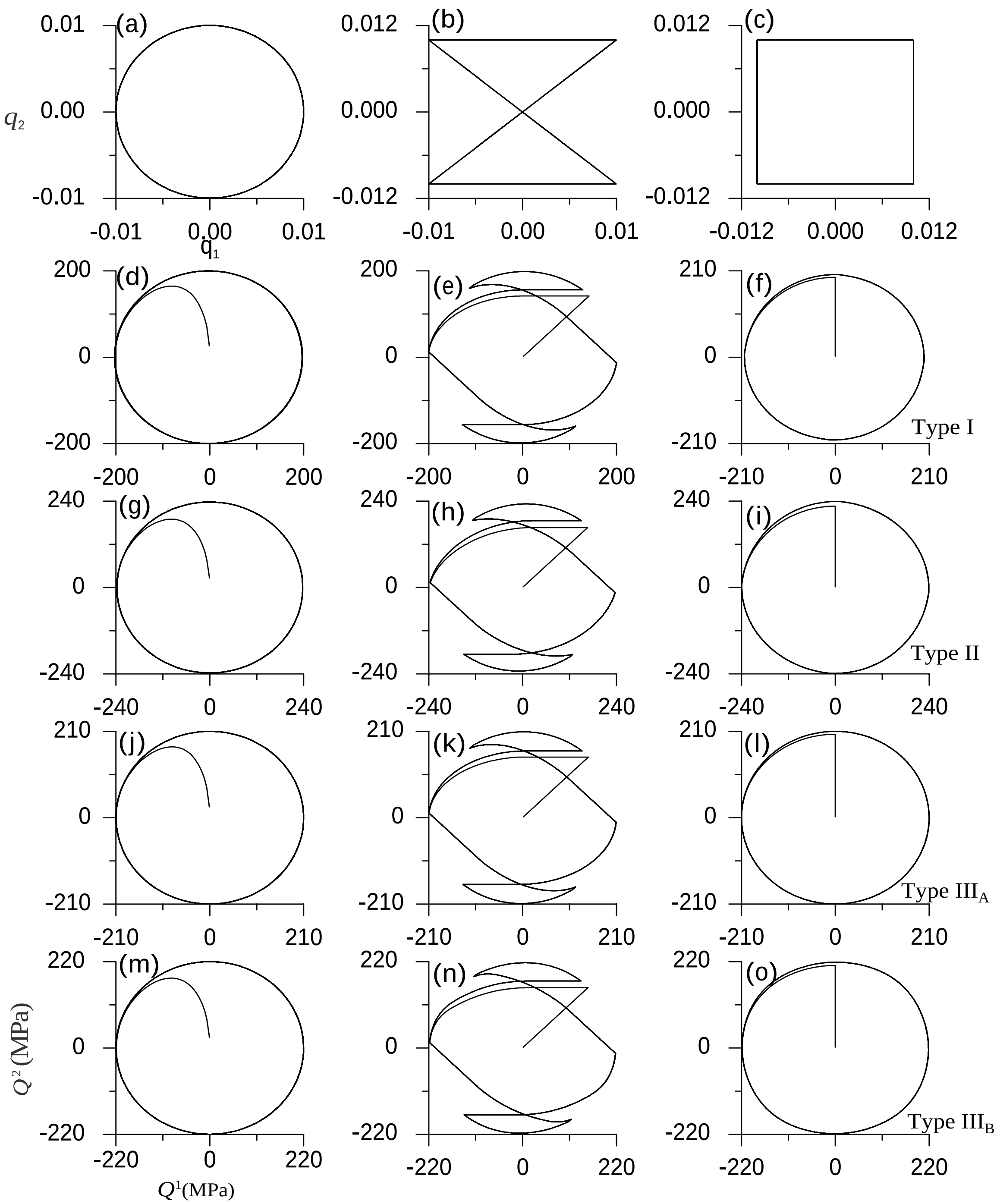

Figure 8 : Under different two-dimensional loading histories the stress paths were shown for the smoothing type I, type II, type IIIA and type IIIB models.

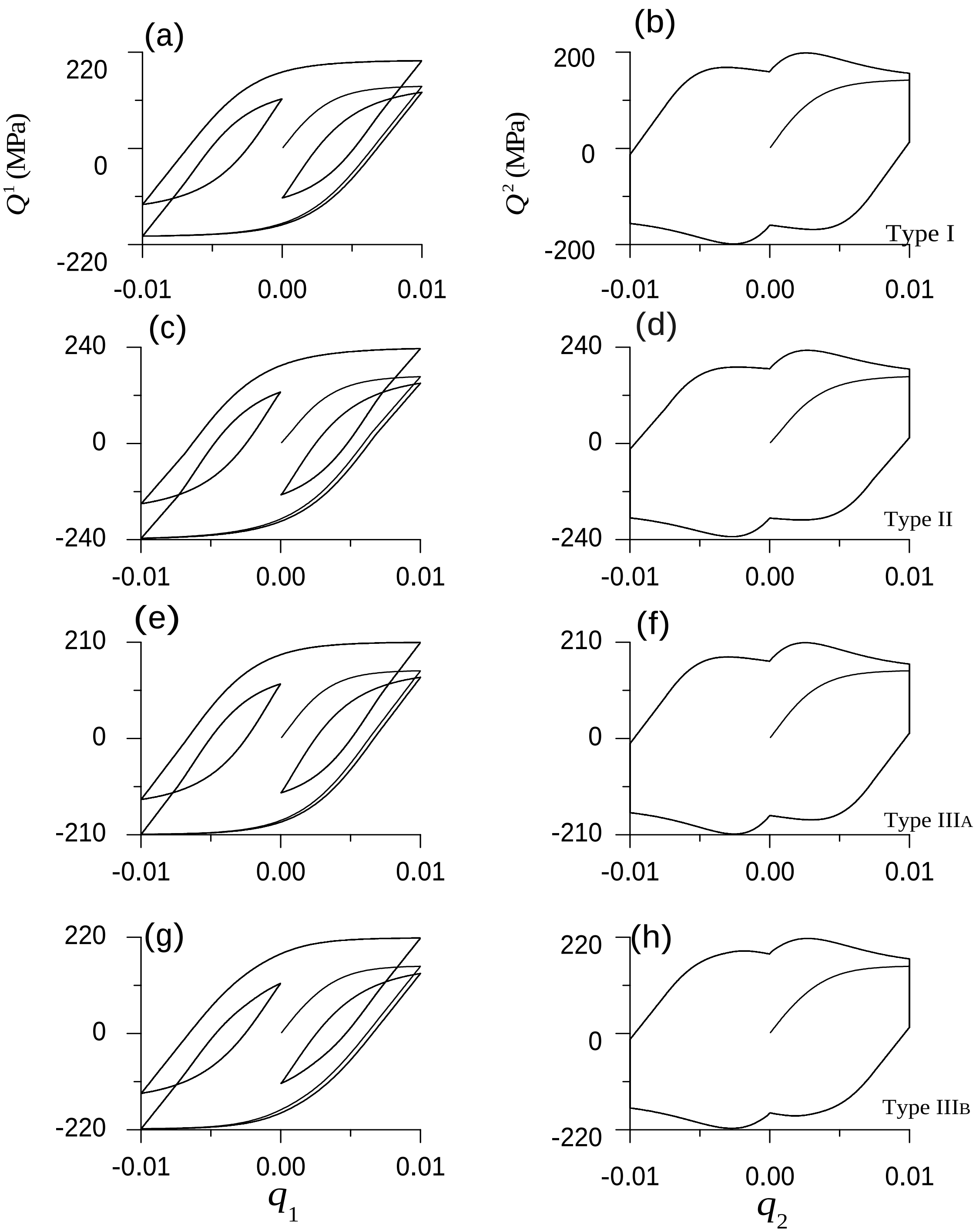

Figure 9 : The hysteretic curves of Q^1 vs. q_1 and Q^2 vs. q_2 were shown for the smoothing type I, type II, type IIIA and type IIIB models under the strain loading path in Fig. 8(b).

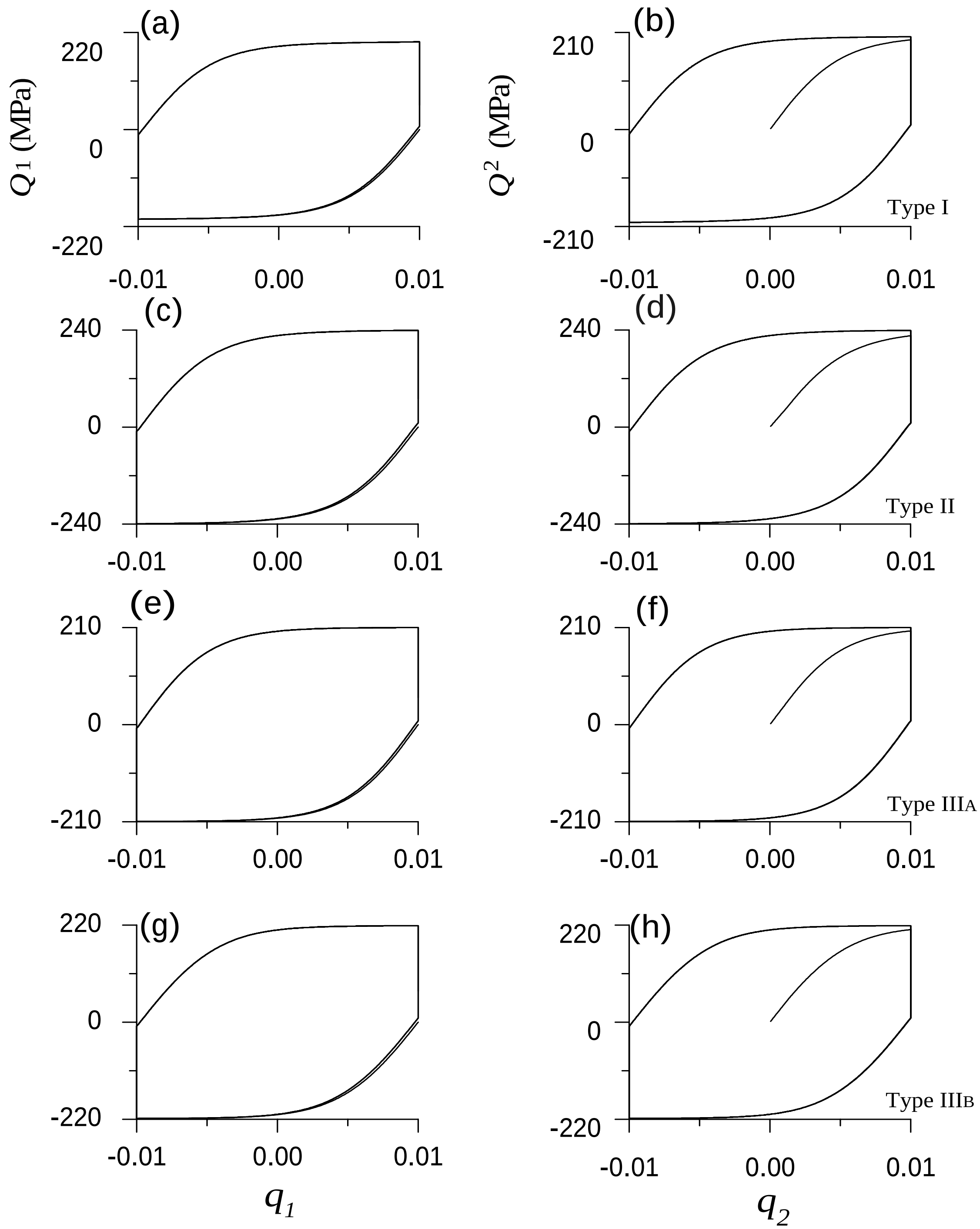

Figure 10 : The hysteretic curves of Q^1 vs. q_1 and Q^2 vs. q_2 were shown for the smoothing type I, type II, type IIIA and type IIIB models under the strain loading path in Fig. 8(c).

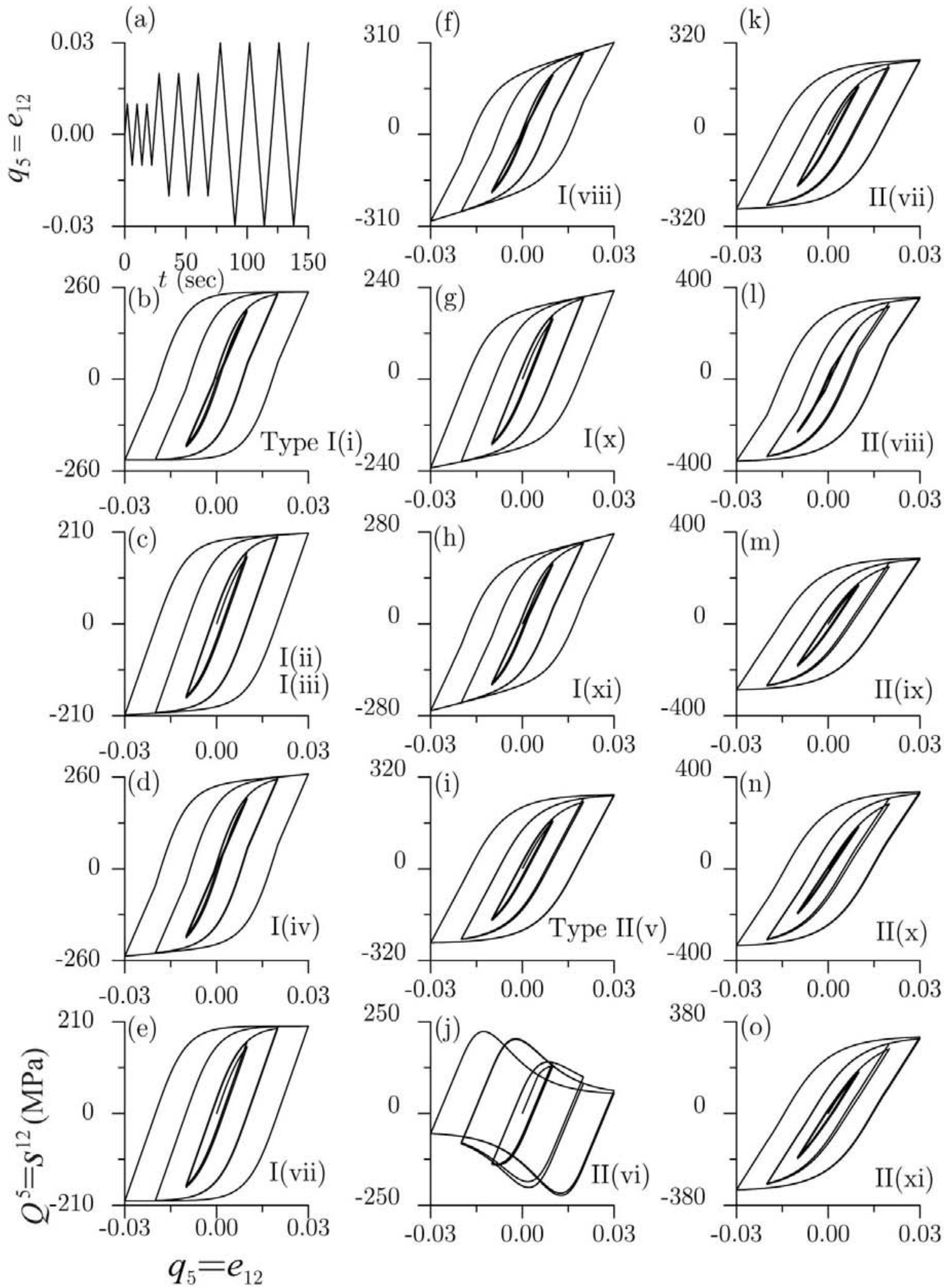

Figure 11 : Under an one-dimensional shear loading history in (a), the hysteretic curves were shown for the smoothing type I and type II models.

Table 5 : The material constants used in Figure 11 for types I and II models

	k_e	k_b	Q_a^0	Q_b^0	r	a_1	a_2	a_3	a_4
Type I(i)	20000	5000	200	20	0.75	0	-4000	4	0
Type I(ii) and (iii)	20000	5000	200	20	0.75	0	0	0	0
Type I(iv)	20000	5000	200	20	0.75	0	4000	4	0
Type I(vii)	20000	5000	200	20	0.75	0.5	-4000	0.2	-10000
Type I(viii)	20000	5000	200	20	0.75	200	-4000	4	0
Type I(x)	20000	5000	200	20	0.75	100	-4000	0.2	0
Type I(xi)	20000	5000	200	20	0.75	100	4000	2	0
Type II(v)	20000	5000	200	40	0.75	0	2000	-0.3	0
Type II(vi)	20000	5000	200	40	-0.1	-125	0	-0.2	10000
Type II(vii)	20000	5000	200	40	0.75	-1	2000	-0.3	20000
Type II(viii)	20000	5000	200	40	0.75	100	-4000	0.5	0
Type II(ix)	20000	5000	200	40	0.75	0	5000	-0.5	0
Type II(x)	20000	5000	200	40	0.75	50	2000	-0.3	0
Type II(xi)	20000	5000	200	40	0.75	50	100	0.3	0

$SO_o(5,1)$ for perfect elastoplasticity with large deformation and a consistency numerical scheme. *Int. J. Non-Linear Mech.*, vol. 34, pp. 1113-1130.

Hong, H.-K.; Liu, C.-S. (1999b): Internal symmetry in bilinear elastoplasticity. *Int. J. Non-Linear Mech.*, vol. 34, pp. 279-288.

Hong, H.-K.; Liu, C.-S. (2000): Internal symmetry in the constitutive model of perfect elastoplasticity. *Int. J. Non-Linear Mech.*, vol. 35, pp. 447-446.

Hong, H.-K.; Liu, C.-S. (2001a): Lorentz group on Minkowski spacetime for construction of the two basic principles of plasticity. *Int. J. Non-Linear Mech.*, vol. 36, pp. 679-686.

Hong, H.-K.; Liu, C.-S. (2001b): Some physical models with Minkowski spacetime structure and Lorentz group symmetry. *Int. J. Non-Linear Mech.*, vol. 36, pp. 1075-1084.

Im, S.; Atluri, S. N. (1987): A study of two finite strain plasticity models: an internal time theory using Mandel's director concept and a combined isotropic-kinematic hardening theory. *Int. J. Plasticity*, vol. 3, pp. 163-191.

Ishlinsky, A. Y. (1954): A general theory of plasticity with linear hardening. *Ukrain. Mat. Zhurnal*, vol. 6, pp. 314-324.

Jiang, Y., Kurath, P. (1996): Characteristics of the Armstrong-Frederick type plasticity models. *Int. J. Plasticity*, vol. 12, pp. 387-415.

Karšaj, I., Sansour, C., Sorić, J. (2005): A new free energy-based model of the kinematic hardening in large strain elastoplasticity. *CMES: Computer Modeling in Engineering & Sciences*, vol. 8, pp. 45-60.

Kurtyka, T.; Życzkowski, M. (1996): Evolution equations for distortional plastic hardening. *Int. J. Plasticity*, vol. 12, pp. 191-213.

Liu, C.-S. (1993): The elastoplastic evolution and stability of materials under mechanical and thermal environments. Ph.D. Dissertation, Department of Civil Engineering, National Taiwan University.

Liu, C.-S. (2001a): The g-based Jordan algebra and Lie algebra with application to the model of visco-elastoplasticity. *J. Marine Sci. Tech.*, vol. 9, pp. 1-13.

Liu, C.-S. (2001b): Cone of non-linear dynamical system and group preserving schemes. *Int. J. Non-Linear Mech.*, vol. 36, pp. 1047-1068.

Liu, C.-S. (2003a): Symmetry groups and the pseudo-Riemann spacetimes for mixed-hardening elastoplasticity. *Int. J. Solids Struct.*, vol. 40, pp. 251-269.

Liu, C.-S. (2003b): Smoothing elastoplastic stress-strain curves obtained by a critical modification of conventional models. *Int. J. Solids Struct.*, vol. 40, pp. 2121-2145.

Liu, C.-S. (2004a): A consistent numerical scheme for the von Mises mixed-hardening constitutive equations. *Int. J. Plasticity*, vol. 20, pp. 663-704.

Liu, C.-S. (2004b): Lie symmetries of finite strain elastic-perfectly plastic models and exactly consistent schemes for numerical integrations. *Int. J. Solids Struct.*, vol. 41, pp. 1823-1853.

Liu, C.-S. (2004c): Internal symmetry groups for the Drucker-Prager material model of plasticity and numerical integrating methods. *Int. J. Solids Struct.*, vol. 41, pp. 3771-3791.

Liu, C.-S.; Chang, C.-W. (2004): Lie group symmetry applied to the computation of convex plasticity constitutive equation. *CMES: Computer Modeling in Engineering & Sciences*, vol. 6, pp. 277-294.

Liu, C.-S.; Chang, C.-W. (2005): Non-canonical Minkowski and pseudo-Riemann frames of plasticity models with anisotropic quadratic yield criteria. *Int. J. Solids Struct.*, vol. 42, pp. 2851-2882.

Liu, C.-S.; Hong, H.-K. (1999): Non-oscillation criteria for hypoelastic models under simple shear deformation. *J. Elasticity*, vol. 57, pp. 201-241.

Liu, C.-S.; Hong, H.-K. (2001): Using comparison theorem to compare corotational stress rates in the model of perfect elastoplasticity. *Int. J. Solids Struct.*, vol. 38, pp. 2969-2987.

Liu, C.-S.; Li, C.-F. (2005): Geometrical numerical algorithms for a plasticity model with Armstrong-Frederick kinematic hardening rule under strain and stress controls. *Int. J. Num. Meth. Eng.*, vol. 63, pp. 1396-1423.

Lubarda, V. A.; Benson, D. J. (2002): On the numerical algorithm for isotropic-kinematic hardening with the Armstrong-Frederick evolution of the back stress. *Comp. Meth. Appl. Mech. Eng.*, vol. 191, pp. 3583-3596.

McDowell, D. L. (1985): An experimental study of the structure of constitutive equations for nonproportional cyclic plasticity. *J. Eng. Mater. Tech. ASME*, vol. 107, pp. 307-315.

McDowell, D. L.; Moosbrugger, J. C. (1992): Continuum slip foundations of elasto-viscoplasticity. *Acta Mech.*, vol. 93, pp. 73-87.

Melan, E. (1938): Zur plastizität des räumlichen kontinuums. *Ing. Archiv. 9*, vol., pp. 116-126.

Moosbrugger, J. C. (1993): Experimental parameter estimation for nonproportional cyclic viscoplasticity: nonlinear kinematic hardening rules for two waspaloy microstructures at 650°C. *Int. J. Plasticity*, vol. 9, pp. 345-373.

Moosbrugger, J. C; McDowell D. L. (1989): On a class of kinematic hardening rules for nonproportional cyclic plasticity. *J. Eng. Mater. Tech. ASME*, vol. 111, pp. 87-98.

Moosbrugger, J. C.; Morrison, D. J. (1997): Nonlinear kinematic hardening rule parameters—direct determination from completely reversed proportional cycling. *Int. J. Plasticity*, vol. 13, pp. 633-668.

Mróz, Z.; Shrivastava, H. P.; Dubey, R. N. (1976): A non-linear hardening model and its application to cyclic loading. *Acta Mech. 25*, vol., pp. 51-61.

Mukherjee, S.; Liu, C.-S. (2003): Computational isotropic-workhardening rate-independent elastoplasticity. *J. Appl. Mech. ASME*, vol. 70, pp. 644-648.

Ohno, N., Wang, J.-D. (1991): Transformation of a nonlinear kinematic hardening rule to a multisurface form under isothermal and nonisothermal conditions. *Int. J. Plasticity*, vol. 7, pp. 879-891.

Ohno, N.; Wang, J.-D. (1993): Kinematic hardening rules with critical state of dynamic recovery, part I: formulation and basic features for ratchetting behavior, part II: application to experiments of ratchetting behavior. *Int. J. Plasticity*, vol. 9, pp. 375-403.

Ohno, N.; Wang, J.-D. (1994): Kinematic hardening rules for simulation of ratchetting behavior. *Eur. J. Mech. A/Solids*, vol. 13, pp. 519-531.

Phillips, A; Lee, C.-W. (1979): Yield surfaces and loading surfaces, experiments and recommendations. *Int. J. Solids Struct.*, vol. 15, pp. 715-729.

Prager, W. (1955): The theory of plasticity: A survey of recent achievements. *Proc. Inst. Mech. Engineers*, vol. 169, pp. 41-57

Prager, W. (1956): A new method of analyzing stresses and strains in work-hardening plastic solids. *J. Appl. Mech. ASME*, vol. 23, pp. 493-496.

Ramaswamy, V. G.; Stouffer, D. C.; Laflen, J. H. (1990): A unified constitutive model for the inelastic uniaxial response of Rene' 80 at temperatures between 538C and 982C. *J. Eng. Mech. ASCE*, vol. 112, pp. 280-286.

Sawyer J. P. G.; Wang, C. H.; Jones, R. (2001): An implicit algorithm using explicit correctors for the kinematic hardening model with multiple back stresses. *Int. J. Num. Meth. Eng.*, vol. 50, pp. 2093-2107.

Trampczyński, W.; Mróz, Z. (1992): Anisotropic hardening model and its application to cyclic loading. *Int. J. Plasticity*, vol. 8, pp. 925-946.

Tseng, N. T.; Lee, G. C. (1983): Simple plasticity model of two-surface type. *J. Eng. Mech. ASCE*, vol. 109, pp. 795-810.

Voyiadjis, G. Z.; Kattan, P. I. (1990): A generalized Eulerian two-surface cyclic plasticity model for finite strains. *Acta Mech.*, vol. 81, pp. 143-162.

Voyiadjis, G. Z.; Kattan, P. I. (1991): Phenomenological evolution equations for the back stress and spin tensors. *Acta Mech.*, vol. 88, pp. 89-111.

Walker, K. P. (1981): Research and development program for non-linear structural modeling with advanced time-temperature dependent constitutive relationships. Report PWA-5700-50, NASA CR-165533.

Wang, C. H.; Hu W.; Sawyer, J. P. G. (2000): Explicit numerical integration algorithm for a class of non-linear kinematic hardening model. *Comp. Mech.*, vol. 26, pp. 140-147.

Watanabe, O.; Atluri, S. N. (1986): Internal time, general internal variable, and multi-yield surface theories of plasticity & creep: a unification of concepts. *Int. J. Plasticity*, vol. 2, pp. 37-57.

Zeeman, E. C. (1964): Causality implies the Lorentz group. *J. Math. Phys.*, vol. 5, pp. 490-493.

Ziegler, H. (1959): A modification of Prager's hardening rule. *Quart. Appl. Math.*, vol. 17, pp. 55-60.